Transportation Research Part C 35 (2013) 263–285

Contents lists available at SciVerse ScienceDirect

Transportation Research Part C

journal homepage: www.elsevier.com/locate/trc

Dynamic stochastic journey time estimation and reliability analysis using stochastic cell transmission model: Algorithm and case studies

Agachai Sumalee [a,*], Tianlu Pan [a], Renxin Zhong [a], Nobuhiro Uno [b], Nakorn Indra-Payoong [c]

[a] Department of Civil and Structural Engineering, The Hong Kong Polytechnic University, Hong Kong Special Administrative Region
[b] Graduate School of Management, Department of Urban Management, Kyoto University, Kyoto, Japan
[c] Faculty of Logistics, Burapha University, Thailand

ARTICLE INFO

Article history:
Received 14 September 2010
Received in revised form 13 November 2012
Accepted 17 November 2012

Keywords:
Dynamic journey travel time distribution
Relative frequency
Probability mass function
Skewness
Travel time reliability

ABSTRACT

This paper proposes a framework for evaluating the distributions of stochastic dynamic link travel time and journey time as well as assessing the journey time reliability. Due to the stochastic nature of the flow profiles, the paper devises a sampling process to estimate the probability mass function (PMF) of the link travel time. This sampling process defines a likelihood concept that measures the probability of the difference between the cumulative stochastic link inflow and outflow profiles to be less than or equal to a prescribed bound. Based on this likelihood measure, the probability mass function (PMF) of the link travel time is evaluated over an appropriate sampling interval. The PMF of the journey time is then evaluated by extending the deterministic nested delay operator to a stochastic version which is defined as a series of "nested" conditional probabilities of the link travel time PMFs along the route. This paper also proposes a method to fit the PMF of the journey time to a class of statistical distribution to determine its skewness, which is useful in the analysis of journey time reliability. The paper then analyzes journey time reliability via the properties of dynamic travel time distributions such as confidence intervals and shape parameters. The proposed algorithm is applied to estimate the stochastic journey time on a freeway corridor from the stochastic cumulative inflow and outflow profiles generated from the stochastic cell transmission model. This methodology is validated with two empirical studies: (i) estimations of journey time distribution and reliability analysis for one short freeway segment in California during a specific time period and (ii) the effects of traffic incidents on journey time reliability for a long expressway corridor of Hanshin expressway (between Osaka and Kobe) in Japan.

1. Introduction

Traffic networks are fragile to both demand and supply uncertainties, especially under incident scenarios and adverse weather conditions. As transportation network is a backbone of a city, the disruption or failure of the transport system may jeopardize the security and welfare of the population. For these reasons, travel time reliability (TTR) has been widely recognized as one of the key performance indicators of transportation networks (Bell, 1999, 2000; Bell and Cassir, 2000; Cassir et al., 2001). Despite its importance, there is no uniform definition of TTR in the sense that what should be precisely en-

* Corresponding author. Tel.: +852 3400 3963; fax: +852 2334 6389.
E-mail addresses: ceasumal@polyu.edu.hk (A. Sumalee), glorious9009@gmail.com (T. Pan), cezhong@gmail.com (R. Zhong), uno@trans.kuciv.kyoto-u.ac.jp (N. Uno), nakorn.ii@gmail.com (N. Indra-Payoong).

0968-090X/$ - see front matter © 2012 Elsevier Ltd. All rights reserved.
http://dx.doi.org/10.1016/j.trc.2012.11.003

tailed by TTR or how it should be made operational. Different indicators for evaluating transport network performance against uncertainties have been proposed ranging from connectivity reliability (Asakura et al., 2003), network vulnerability (Berdica, 2002; Taylor et al., 2006), capacity reliability (Chen et al., 2002; Sumalee and Kurauchi, 2006), travel time reliability (Asakura and Kashiwadani, 1991), total travel time reliability (Clark and Watling, 2005), to demand satisfaction measure (Heydecker et al., 2007). Different indices are appropriate for different purposes and circumstances. For instance, the connectivity reliability and network vulnerability were mainly devised for an extreme condition of the network, e.g. after disaster or emergency evacuation. On the other hand, the journey time reliability deals with recurrent performance of the network.

Journey time reliability, which describes the degree of stability of journey time, plays an important role in travelers' route choice and departure time choice behavior. The variation of journey time is caused by both demand uncertainties and stochastic capacities (e.g. due to weather, incident, or road-maintenance). Existing studies on travel time reliability primarily focus on devising indices to quantify the level of journey time uncertainty (or reliability) in a static network model (Cassir et al., 2001; Bell, 2000; Bell and Cassir, 2002; Lo et al., 2006; Clark and Watling, 2005). What these measures have in common is that the longer-tailed the travel time distribution is on a particular time-of-day (TOD)/day-of-the-week (DOW), the more unreliable travel time on a freeway network or corridor (van Lint et al., 2008). Furthermore, the propagation of delay and uncertainty through the traffic network dynamically and spatially can be naturally observed. The level of travel time reliability and uncertainty, hence, should be assessed dynamically. Nevertheless, recent research suggests that even both the mean and variance of the travel time are obtained, still they should be used and interpreted with some reservations when telling the travel time unreliability, since they only account for a part of the costs of unreliability (van Lint et al., 2008; Cassir et al., 2001). The skewness of the travel time distribution plays an important role in travel time unreliability. In a word, a central element of the dynamic journey time reliability is the evaluation of dynamic travel time distribution.

Much research work has been dedicated recently to the study of the way travelers react to the shape of the the distribution of stochastic dynamic link travel time (DDTT) (see e.g. Bates et al., 2001; Pattanamekar et al., 2003; Chang et al., 2005; Huang and Gao, 2012). However, less attention has been paid to developing tools for estimating the DDTT itself (Sun et al., 2008). In the context of optimal routing, most of the algorithms consider the expected value of link travel-time as a sufficient statistic for the problem and produce least expected travel-time paths, i.e. travelers are assumed to choose their routes with minimum expected costs (Fu and Rilett, 1998; Miller-Hooks and Mahmassani, 2000; Huang and Gao, 2012). Further more, these papers presumed fully knowledge on the distributions of link travel times. The route travel times were then obtained recursively using the nested delay operator under the umbrella of time-dependent network. Therefore, it is instructive and important to develop sound evaluation methods for DDTT. Nevertheless, constructing the distribution of dynamic route journey time from the distributions of link travel times is a difficult task that enforces several assumptions in transportation literature (Miller-Hooks and Mahmassani, 2000), e.g. independent link travel times in Jula et al. (2008).

Conventionally, there are several methods to calculate link travel (or journey) time: evaluation from advanced surveillance systems: video image processing, automatic vehicle identification, smart phone/GPS tracking, probe vehicles using traffic flow theory and/or statistical methods (see e.g. Petty et al., 1998; Coifman, 2002; Dion and Rakha, 2006; Haghani et al., 2010; Herrera et al., 2010; Sumalee and Wang, in press), dynamic traffic assignment models (see e.g. Peeta and Ziliaskopoulos, 2001; Wen, 2008), statistical and computational intelligence (CI) based approaches (see e.g. Wu et al., 2004; van Lint et al., 2005; van Lint, 2008; Jula et al., 2008; Karlaftis and Vlahogianni, 2011), and dynamic traffic flow propagation based matching algorithms (see e.g. Lo and Szeto, 2002; Carey and Ge, 2012). All these methods can be regarded as fitting different types of models to observed data at individual sites. In this sense, major techniques for (short-term) travel-time evaluation are of three major categories in transportation literature: parametric methods (e.g. linear regression, time series models, dynamic traffic assignment models, Kalman filtering techniques), nonparametric statistical methods (e.g. neural network models, simulation models, Bayesian models, support vector regression), and hybrid integration methods. The statistical approaches have more solid and widely accepted mathematical foundations than the CI based approaches (Karlaftis and Vlahogianni, 2011). On the other hand, the statistical approaches frequently fail when dealing with complex and highly nonlinear data and suffer from the curse of dimensionality. As highlighted by Karlaftis and Vlahogianni (2011), the CI based approaches, combining techniques from machine learning, adaptation, evolution and fuzzy logic to create intelligent models to emerge unstructured data by following some performance indexes, may outperform the statistical approaches. However, we may point out that abnormal traffic patterns caused by non-recurrent congestion or incidents may deteriorate the performance of these models (Fei et al., 2011). Some of these methods do not work well under demand and supply uncertainties. The DTA based approaches would suffer from the disadvantages of the accuracy of network loading models and scalability. Nevertheless, most of these methods provide mean and variance of the dynamic travel time only, which may not be sufficient for a broad range of applications. Only few works have been dedicated to evaluate stochastic travel time distributions analytically (Kharoufeh and Gautam, 2004). The approach proposed by Kharoufeh and Gautam (2004) implicitly captures the time dependence of stochastic vehicle speed in terms of partial differential equations. When the environmental process is assumed to be a continuous-time Markov chain (CTMC), an explicit matrix equation for the stochastic dynamic link travel time distribution can be obtained. Although the technique presented in Kharoufeh and Gautam (2004) provides an analytical result for the link travel-time distribution, the proposed approach depends on some ingenuities in determining the appropriate selection of transition rates for the CTMC and the vehicle speed function. This renders that the proposed approach cannot deduce general explicit expressions for the moments of the random travel time. Nevertheless, this method is very computationally demanding and is not ready to be extended to capture route travel (or journal) time distributions.

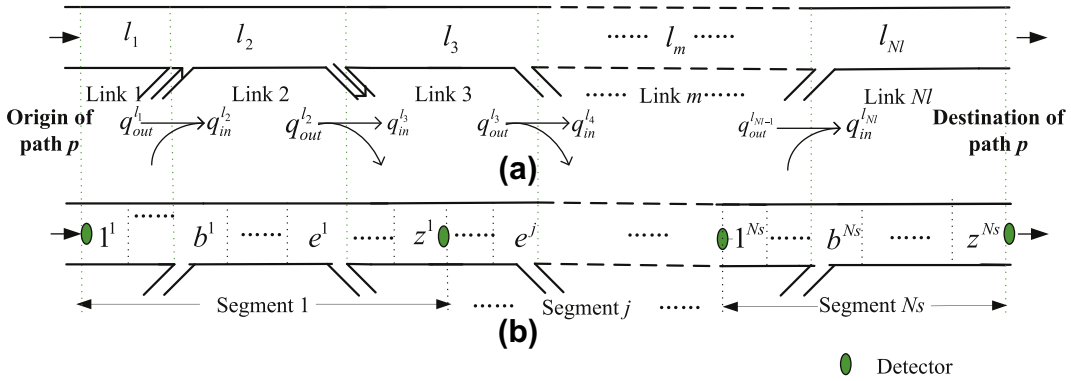

Fig. 1. The relationship of the segment used in SCTM and the link used in travel time estimation.

For the deterministic dynamic flow model, to evaluate the travel time via the traffic flow propagation, the principle of first-in-first-out (FIFO) of traffic flows is utilized, i.e. comparing the cumulative inflow and cumulative outflow profiles in which the exit time for traffic entering the link at time t is the time when the cumulative outflow of that link is equal to the cumulative inflow up to time t. This paper extends the FIFO concept to evaluate travel time distribution based on the stochastic cumulative inflow and outflow curves. Generally speaking, any stochastic cumulative inflow and outflow can be utilized as inputs to the proposed algorithm to evaluate stochastic travel time distribution as long as the FIFO principle is satisfied in the sense of "almost sure". In particular, we adopt the stochastic cell transmission model (SCTM) proposed by Sumalee et al. (2011) as network loading model to generate these flow profiles from the traffic data collected by point sensors so as to capture the randomness in both demand and supply sides. To evaluate the journey time, a long freeway corridor[1] is divided into several links such that the on-ramps are located at the first cells of the links while the off-ramps are located at the last cells. For each of the entry time interval the algorithm will evaluate the likelihood of the link travel time by calculating the probability of the mapping error, i.e. the difference between the stochastic cumulative inflow at the entry time and the stochastic cumulative outflow at each of the sampled exit times, to be less than a prescribed bound. Thus, for a given entry time the probability of each of the future time interval to be the exit time of this entry time can be calculated. The probability mass function (PMF) of the exit time for each entry time can then be evaluated (Miller-Hooks and Mahmassani, 2000). The journey time can be evaluated by extending the nested delay operator to the stochastic environment by using the Bayes' rule. Distribution fitting technique will be applied to capture the skewness and distribution of dynamic journey time. Travel time reliability will then be evaluated by examining different reliability indexes using the distribution of dynamic journey time obtained.

This paper is structured into five further sections. The next section provides necessary preliminaries on the dynamic travel time estimation from the exit-flow model and a brief introduction of the SCTM. Then, the third section presents the proposed algorithm for estimating the PMF of link exit time from the dynamic stochastic flow outputs of the SCTM. The fourth section explains the derivation of the stochastic path journey time from the PMF of link exit time and introduces the buffer-time index for reliability evaluation. The proposed algorithm is then tested with two empirical case studies in Section 5. The first case study is a short freeway segment using the historical data of a month from the performance measurement system (PeMS) database. The second case study is a long Japanese expressway corridor (12 km). The final section then concludes the paper.

2. Preliminaries

2.1. Deterministic link travel time estimation from an exit-flow model and journey time estimation

Consider a path on a long freeway corridor as depicted in Fig. 1. Firstly, the path is divided into several links by the on-ramps and the off-ramps along the corridor such as link l_m, and as illustrated in Fig. 1a, the path is partitioned into Nl links. Segment is a concept used in SCTM, with each segment consisting of several cells and having the neighbor detectors as its boundaries. The same freeway corridor represented by Ns segments is shown as Fig. 1b. With these concepts, we introduce the link travel time evaluation under a macroscopic continuous-time deterministic dynamic traffic flow model. The flow propagation equation for link l_m can be expressed as follows:

$$C^{l_m}_{in}(t) = C^{l_m}_{out}(\tau_{l_m}(t)), \tag{1}$$

[1] A path concerned in this paper mainly refers to a freeway corridor. However, the proposed method is not limited to freeways, see e.g. Zhong (2011) for the extension to evaluate travel time distribution for arterials.

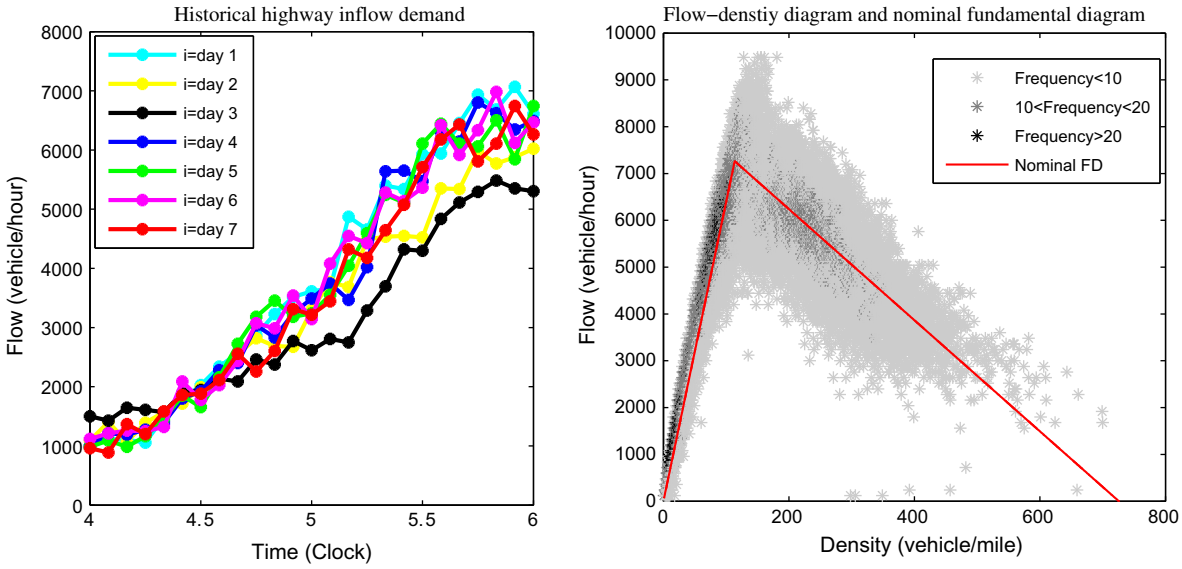

Fig. 2. Stochastic inflow demand and fundamental diagram.

where $\tau_{l_m}(t)$ is the exit time from l_m for a vehicle that enters this link at time t,[2] and $C_{in}^{l_m}(t)$ and $C_{out}^{l_m}(\tau_{l_m}(t))$ are the cumulative inflow and outflow volumes at the entry and exit times of this link, respectively. The time–flow consistency equation in (1) is applicable on condition that the FIFO principle holds. The deterministic link travel time $\beta_{l_m}(t)$ can be defined ass

$$\beta_{l_m}(t) = \tau_{l_m}(t) - t. \tag{2}$$

The journey time of path p is then defined by the nested delay operator with exit time $\tau_{l_m}(t)$ $(\forall l_m \in p)$ of all the links on the path as:

$$\eta_p(t) = \tau_{l_{NI}}(\cdots \tau_{l_m}(\cdots \tau_{l_1}(t))) - t, \tag{3}$$

where the exit time from link m is the entry time to link $m+1$.

2.2. The stochastic cell transmission model (SCTM)

We adopt the stochastic cell transmission model (SCTM) proposed by Sumalee et al. (2011) as the network loading model to furnish the stochastic flow profiles for the evaluation of travel time distributions by extending (1). The SCTM considers stochastic characteristics of the fundamental diagram (uncertain flow–density relationship) and admits the stochastic travel demand as exogenous input as illustrated in Fig. 2. For the supply side, the means and variances of different parameters (i.e. free-flow speed, jam-density, critical-density, and backward-wave speed) which govern the fundamental diagram are calibrated based on the statistics of the observed data (e.g. the grey dots in the right-hand side of Fig. 2) for each section equipped with detectors. The SCTM defines the random inflows (uncertain demand) as well as random parameters of the fundamental flow–density diagram (uncertain supply functions) as boundary variables. It accepts the means and variances of the boundary variables as exogenous inputs, and then calculates the means and variances of the traffic densities, outflow of the freeway segment and probabilities of its operational modes.[3] as outputs based on the measured boundary conditions as illustrated in Fig. 3 To be specific, at each simulation time step, the stochastic flow propagation between adjacent cells under each mode can be determined by the flow–density relationship (see Sumalee et al. (2011) for details). Each of these stochastic flow profiles is associated with a certain probability corresponding to an operational mode. The flow propagated from upstream to downstream cell in the next time step is a mixture distribution of the stochastic flows of the operational modes. Detailed discussion can be found in Sumalee et al. (2011) and is omitted here for brevity. For the purpose of calculating dynamic travel time distribution, we need also to obtain the distributions of dynamic link inflow and outflow from the simulation outputs of the SCTM as discussed in Sumalee et al. (2011).

[2] It is important to recognize that this exit time definition is time-and-flow-driven, i.e. the exit time is related to both travelers and their entry time. It may be not rigorous with zero arrival or departure flow-rates if the exit time is regarded as time-driven only, e.g. travel time of link a at 8:00 am may be not well defined if there is no entry flow to the link. A discussion on this "no flow" issue and its extension is discussed in Zhong (2011) for signal junction applications wherein flows can be zero due to signal effects.

[3] For a short freeway segment, the SCTM defines five operational modes with respect to different traffic conditions, location and movement of the wavefront.

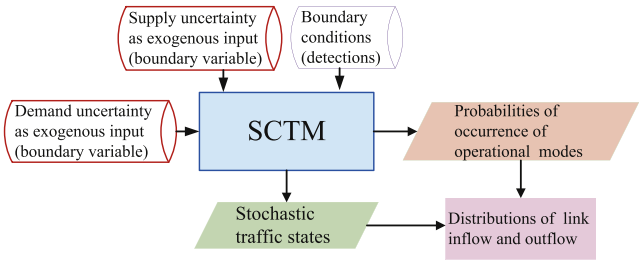

Fig. 3. Block diagram representation of the stochastic cell transmission model.

3. Evaluation of stochastic dynamic journey time

3.1. Probabilistic mass function and normalization of the link travel time

Since the cumulative inflow and outflow are both random processes, the FIFO principle based travel time estimation method is not directly applicable.[4] Nevertheless, the FIFO principle is extended here to estimate the probability of travel time to be a certain value. For a given entry time, this extension estimates the probability of each of the future time interval to be the exit time of this entry time. This probability is defined according to the likelihood that the difference between the cumulative inflow and the cumulative outflow at a future time step is less than a prescribed bound. To apply this concept by incorporating the outputs from the SCTM, we discretize the continuous time into small discrete time intervals. By the SCTM, the distributions of inflow rate $q_{in}^{l_m}(k)$ and outflow rate $q_{out}^{l_m}(k)$ of link l_m can be obtained. Based on the distributions of inflow rate $q_{in}^{l_m}(k)$ and outflow rate $q_{out}^{l_m}(k)$ of link l_m, the corresponding cumulative inflow and outflow distributions can easily be evaluated.[5] Assume $C_{in}^{l_m}(k) \cong f_{Cin}\left(\overline{C}_{in}^{l_m}(k), \sigma_{C_{in}^{l_m}}(k)\right)$, where $f_{Cin}(\cdot)$ denotes a certain statistical distribution, $\overline{C}_{in}^{l_m}(k)$ denotes the mean value, and $\sigma_{C_{in}^{l_m}}(k)$ denotes the standard deviation of the cumulative link inflow. Similarly, the cumulative link outflow is defined as $C_{out}^{l_m}(k) \cong f_{Cout}\left(\overline{C}_{out}^{l_m}(k), \sigma_{C_{out}^{l_m}}(k)\right)$. The probability of the time step k' to be the exit time for vehicles entering the link at time k (i.e. the entry time $ET = k$) can be written as: $\Pr\left(C_{in}^{l_m}(k) = C_{out}^{l_m}(k')\right)$. However, this probability is not well defined. Thus, the likelihood for the time step k' to be the exit time (or $k' - k$ to be travel time) for vehicles entering the link at time k is proposed as:

$$P'_{k'|k} = \Pr\left(-\varepsilon \leqslant C_{out}^{l_m}(k') - C_{in}^{l_m}(k) \leqslant \varepsilon | ET = k\right), \tag{4}$$

where $\varepsilon \in R^+$ denotes a pre-defined positive small number.[6] In the empirical studies, we will show that the travel time distribution is robust (non-sensitive) to the choice of ε.

To interpret the above likelihood, we define $e_k(k') = C_{out}^{l_m}(k') - C_{in}^{l_m}(k)$ as the matching error which measures the difference between the cumulative inflow and outflow distributions. Eq. (4) is then equivalent to $P'_{k'|k} = \Pr(-\varepsilon \leqslant e_k(k') \leqslant \varepsilon | ET = k)$. We can simplify the calculation of $e_k(k')$ as:

$$\begin{aligned} e_k(k') &= C_{out}^{l_m}(k') - C_{in}^{l_m}(k) = \sum_{x=1}^{k'-1} q_{out}^{l_m}(x)\Delta t - \sum_{x=1}^{k-1} q_{in}^{l_m}(x)\Delta t = \sum_{x=k}^{k'-1} q_{out}^{l_m}(x)\Delta t - \left(-\sum_{x=1}^{k-1} q_{out}^{l_m}(x) + \sum_{x=1}^{k-1} q_{in}^{l_m}(x)\right)\Delta t \\ &= \sum_{x=k}^{k'-1} q_{out}^{l_m}(x)\Delta t - \sum_{i=1}^{NC_{l_m}} \rho_i^{l_m}(k) s_i^{l_m}, \end{aligned} \tag{5}$$

where Δt is the interval of the discretized time step, NC_{l_m} is the number of cells on link l_m, $\rho_i^{l_m}(k)$ is the density of the ith cell on link l_m at time k, and $s_i^{l_m}$ is the length of the cell. Note that $s_i^{l_m}$ and Δt are constants meanwhile the link outflow profile and cell densities are normally distributed by assumption, the matching error is normally distributed.[7] Thus, it is sufficient for us to obtain the mean and variance of Eq. (5) so as to evaluate the probability defined by Eq. (4). The expectation of Eq. (5) is

[4] If a macroscopic traffic flow model is adopted to simulate the traffic dynamics, the FIFO principle needs to be fulfilled by the underlying traffic flow model. In this paper, SCTM is utilized as the network loading model. Under the deterministic CTM, the FIFO principle will be fulfilled if the cell length l_i is chosen such that $v_{f,i}T_s \leqslant l_i$ where $v_{f,i}$ is the free flow speed of cell i, and T_s is the simulation time increment. This condition cannot always be satisfied in the SCTM framework since mathematically the free-flow speed $v_{f,i}$ can be anything along its distribution. Nevertheless, certain concept that is similar to the "almost sure (or with probability one)" in stochastic analysis can be adopted to redefine this condition. The probabilistic version of the FIFO condition in the SCTM framework is roughly defined as $\Pr(v_{f,i}T_s \leqslant l_i) \geqslant \chi$, where χ is a positive real number which satisfies $1 - \epsilon < \chi < 1$ for a small real number ϵ. We may choose χ very close to 1, such that $\Pr(v_{f,i}T_s \leqslant l_i) \approx 1$, i.e. the event $v_{f,i}T_s \leqslant l_i$ is almost sure. In the empirical studies, the cell lengths are defined according to this condition. In other word, the FIFO is well satisfied in the sense of "almost sure" in the SCTM formulation.

[5] Note that in Eq. (5), due to the discretization, cumulative flows at time step k are calculated up to $k - 1$. This implies that $q_{in}^{l_m}(k)$ is regarded as the inflow rate during the time interval $[k, k+1)\triangle t$. The same logic is applied to the calculation of cumulative outflow.

[6] In our empirical studies, if not else specified, the value ε is 1 by default.

[7] Please see Appendix A.1 for details.

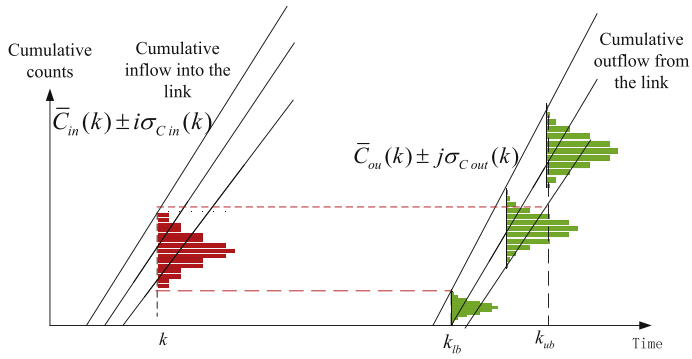

Fig. 4. An illustration of the *sampling* region.

$$E(e_k(k')) = \sum_{x=k}^{k'-1} \Delta t \cdot E\left(q_{out}^{l_m}(x)\right) - \sum_{i=1}^{NC_{l_m}} s_i^{l_m} \cdot E\left(\rho_i^{l_m}(k)\right). \tag{6}$$

If the above random variables are uncorrelated, we can obtained the variance of $e_k(k')$ easily by the additive of independent normal variables. However, the variance is not additive in general due to the correlation. Nevertheless, we can make use of the covariance matrix[8] of the corresponding vector (augmented by the above random variables) obtained from the SCTM to proceed with the variance evaluation which is discussed in detail in Appendix A.1 of the paper. As it will be shown in the empirical study, improvement contributed by incorporating the covariance matrix (i.e. considering the correlation) to dynamic travel time distribution is not significant.

To evaluate the probability mass function (PMF) of the link travel time for an entry time k, it is necessary to evaluate the probability in Eq. (4) against all possible exit time $k' > k$. This is considered impractical and unnecessary (Miller-Hooks and Mahmassani, 2000). The proposed method will only evaluate the probability defined by Eq. (4) against a certain interval of the exit time, say $[k_{lb}\ k_{ub}]$, which is defined by the lower-bound k_{lb} and upper-bound k_{ub} as:

$$\begin{aligned} k_{lb} &= \min\left\{k' :\ \min\left\|\left(\bar{C}_{in}^{l_m}(k) - i\sigma_{C_{in}^{l_m}}(k)\right) - \left(\bar{C}_{out}^{l_m}(k') + j\sigma_{C_{out}^{l_m}}(k')\right)\right\|\right\}, \\ k_{ub} &= \min\left\{k' :\ \min\left\|\left(\bar{C}_{in}^{l_m}(k) + i\sigma_{C_{in}^{l_m}}(k)\right) - \left(\bar{C}_{out}^{l_m}(k') - j\sigma_{C_{out}^{l_m}}(k')\right)\right\|\right\}, \end{aligned} \tag{7}$$

where i, j can be selected as small positive integers (non-integers are also acceptable) which can be adjusted such that there is no overlapping between the two curves $\bar{C}_{in}^{l_m}(k) - i\sigma_{C_{in}^{l_m}}(k)$ and $\bar{C}_{out}^{l_m}(k') + j\sigma_{C_{out}^{l_m}}(k')$ (which in turn implies $k' > k$), (see Fig. 4).[9] In Section 5, a comparison of journey time results by assigning different values to i, j will be conducted. It is found that the algorithm is robust to the choice of i, j.

Following the sampling technique described by Eqs. (4)–(7), a series of $P'_{k'|k}$, which describe the likelihood of k' to be the exit time index for entry time k (whereas the link travel time is defined as $(k' - k)\Delta t$), can be obtained. As the summation of the probabilities $\sum_{k_{lb}}^{k_{ub}} P'_{k'|k}$ may not be equal to 1, the relative frequency is introduced to normalize the probabilities. For a vehicle entering link l_m at time k, the relative frequency $P_{k'|k}$ is defined as:

$$P_{k'|k} = \frac{P'_{k'|k}}{\sum_{k_{lb}}^{k_{ub}} P'_{k'|k}}, \quad \forall\ k' \in [k_{lb}, k_{ub}]. \tag{8}$$

From the normalized probabilities, the PMF of the link exit time for vehicles entering at time index k is constructed as shown in Fig. 5. Each bar on the upper plot represents $P_{k'|k}$, and the lower plot denotes the corresponding cumulative mass function (CMF).

3.2. Probabilistic mass function of path journey time

Consider a path from link l_1 to link l_{Nl} as depicted in Fig. 6. To trace the path travel time distribution for vehicles entering the origin at time step k, we extend the nested delay operator to the stochastic case. The relative frequency of time-step τ^{Nl} to be the exit time from the destination of the path for vehicles entering the origin at time step k is derived as follows:

[8] If X is a random vector with n components, the matrix $Var(X) = E((X - E(X))(X - E(X))^T)$ is the covariance matrix.

[9] Detailed analysis on the choice of i, j is given in Appendix A.2. In the empirical studies, if not specified, i, j are set to be 3.

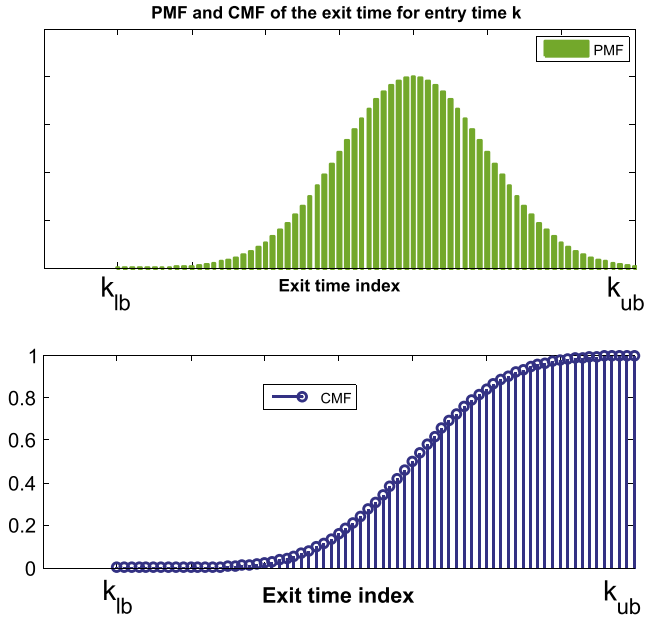

Fig. 5. The PMF and corresponding CMF respect to exit time index for entry time index k.

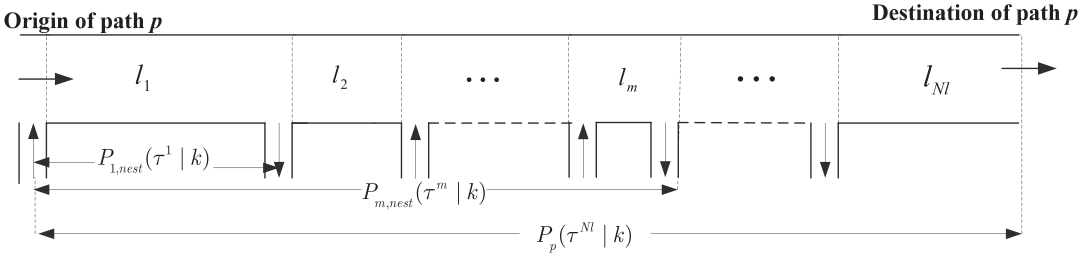

Fig. 6. Nested delay operator for a path with Nl links.

$$
\begin{aligned}
&P_{1,nest}(\tau^1|k) = P_1(\tau^1|k), \quad \tau^1 \in \left[k_{lb}^{l_1}, k_{ub}^{l_1}\right],\\
&P_{2,nest}(\tau^2|k) = \sum_{\tau^1=k_{lb}^{l_1}}^{k_{ub}^{l_1}} P_2(\tau^2|\tau^1) P_{1,nest}(\tau^1|k), \quad \tau^2 \in \left[\left(k_{lb}^{l_1}\right)_{lb}^{l_2}, \left(k_{ub}^{l_1}\right)_{ub}^{l_2}\right],\\
&\vdots\\
&P_{m,nest}(\tau^m|k) = \sum_{\tau^{m-1}=\left(\left(k_{lb}^{l_1}\right)\cdots\right)_{lb}^{l_{m-1}}}^{\left(\left(k_{ub}^{l_1}\right)\cdots\right)_{ub}^{l_{m-1}}} P_m(\tau^m|\tau^{m-1}) P_{m-1,nest}(\tau^{m-1}|k), \quad \tau^m \in \left[\left(\left(k_{lb}^{l_1}\right)\cdots\right)_{lb}^{l_m}, \left(\left(k_{ub}^{l_1}\right)\cdots\right)_{ub}^{l_m}\right],\\
&\vdots\\
&P_p(\tau^{Nl}|k) = \sum_{\tau^{Nl-1}=\left(\left(k_{lb}^{l_1}\right)\cdots\right)_{lb}^{l_{Nl-1}}}^{\left(\left(k_{ub}^{l_1}\right)\cdots\right)_{ub}^{l_{Nl-1}}} P_{Nl}(\tau^{Nl}|\tau^{Nl-1}) P_{Nl-1,nest}(k^{Nl-1}|k),
\end{aligned}
\tag{9}
$$

where $k_{lb}^{l_1}, k_{ub}^{l_1}$ can be defined according to Eq. (7). Other bounds can be defined recursively as:

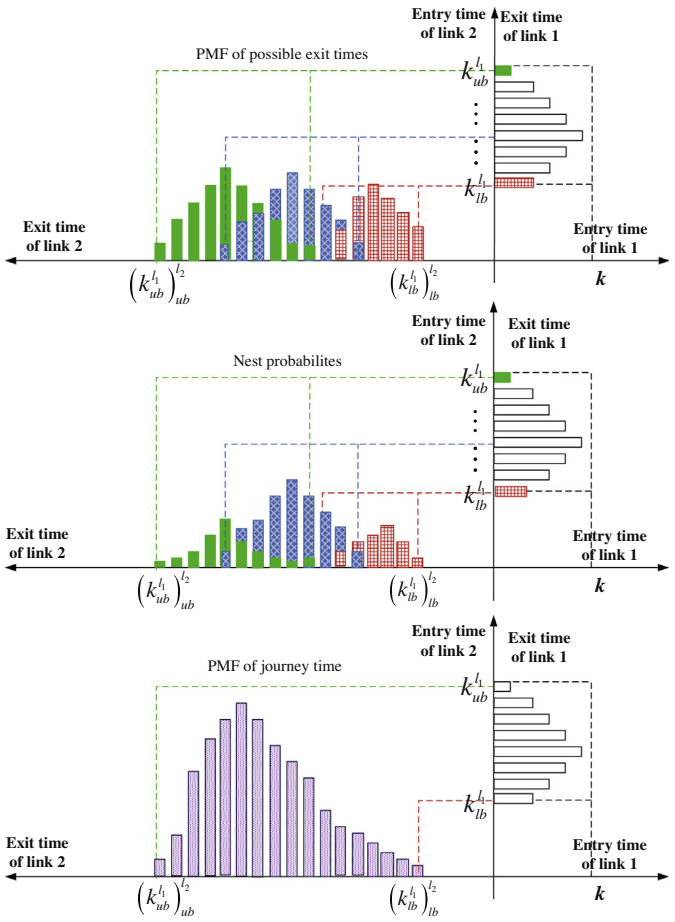

Fig. 7. Demonstration of nested delay operator for a path with two links.

$$
\begin{aligned}
\left(k_{lb}^{l_1}\right)_{lb}^{l_2} &= \min\left\{k' : \left\|\left(\overline{C}_{in}^{l_2}\left(k_{lb}^{l_1}\right) - i\sigma_{C_{in}^{l_2}}\left(k_{lb}^{l_1}\right)\right) - \left(\overline{C}_{out}^{l_2}(k') + j\sigma_{C_{out}^{l_2}}(k')\right)\right\| \leqslant \varepsilon_s\right\},\\
\left(k_{ub}^{l_1}\right)_{ub}^{l_2} &= \min\left\{k' : \left\|\left(\overline{C}_{in}^{l_2}\left(k_{ub}^{l_1}\right) + i\sigma_{C_{in}^{l_2}}\left(k_{ub}^{l_1}\right)\right) - \left(\overline{C}_{out}^{l_2}(k') - j\sigma_{C_{out}^{l_2}}(k')\right)\right\| \leqslant \varepsilon_s\right\},\\
&\vdots\\
\left(\left(k_{lb}^{l_1}\right)\cdots\right)_{lb}^{l_m} &= \min\left\{k' : \left\|\left(\overline{C}_{in}^{l_m}\left(\left(\left(k_{lb}^{l_1}\right)\cdots\right)_{lb}^{l_{m-1}}\right) - i\sigma_{C_{in}^{l_m}}\left(\left(\left(k_{lb}^{l_1}\right)\cdots\right)_{lb}^{l_{m-1}}\right)\right) - \left(\overline{C}_{out}^{l_m}(k') + j\sigma_{C_{out}^{l_m}}(k')\right)\right\| \leqslant \varepsilon_s\right\},\\
\left(\left(k_{ub}^{l_1}\right)\cdots\right)_{ub}^{l_m} &= \min\left\{k' : \left\|\left(\overline{C}_{in}^{l_m}\left(\left(\left(k_{ub}^{l_1}\right)\cdots\right)_{ub}^{l_{m-1}}\right) + i\sigma_{C_{in}^{l_m}}\left(\left(\left(k_{ub}^{l_1}\right)\cdots\right)_{ub}^{l_{m-1}}\right)\right) - \left(\overline{C}_{out}^{l_m}(k') - j\sigma_{C_{out}^{l_m}}(k')\right)\right\| \leqslant \varepsilon_s\right\},
\end{aligned}
\tag{10}
$$

where the superscript l_m is used to denote the link number.

Fig. 7 demonstrates the calculation process of nested delay operator from $P_1(\tau^1|k)$ to $P_2(\tau^2|k)$ for vehicles entering link 1 at time index k. By the proposed PMF definition of the exit time, we can first obtain a series of blank bars in the right-hand side of the figure. Each time index τ^1 (corresponding to each blank bar in the right-hand side of the figure) between $\left[k_{lb}^{l_1}, k_{ub}^{l_1}\right]$ results in a PMF $P_2(\tau^2|\tau^1)$ according to the exit time probability defined by Eqs. (4) and (8). For example, in the upmost part of Fig. 7, time index $\tau^1 = k_{lb}^{l_1}$ yields a PMF $P_2(\tau^2|\tau^1)$ depicted in red[10] bars while $\tau^1 = k_{ub}^{l_1}$ results in a PMF $P_2(\tau^2|\tau^1)$ in green color. Therefore, for vehicles entering link 1 at k, the potential interval of exit time from link 2 is extended to $\left[\left(k_{lb}^{l_1}\right)_{lb}^{l_2}, \left(k_{ub}^{l_1}\right)_{ub}^{l_2}\right]$, e.g. the left-hand side of the upmost part of Fig. 7. We then apply the Bayes' rule defined by Eq. (9) to obtained the nested probabilities, i.e. $P_2(\tau^2|\tau^1)P_{1,nest}(\tau^1|k)$ depicted in the middle part of the figure. Finally, the PMF of journey time for vehicles entering link 1 at time index k is given by the summation of the nested probabilities which is depicted in the lower part of Fig. 7. In Appendix A.3

[10] For interpretation of color in Fig. 7, the reader is referred to the web version of this article.

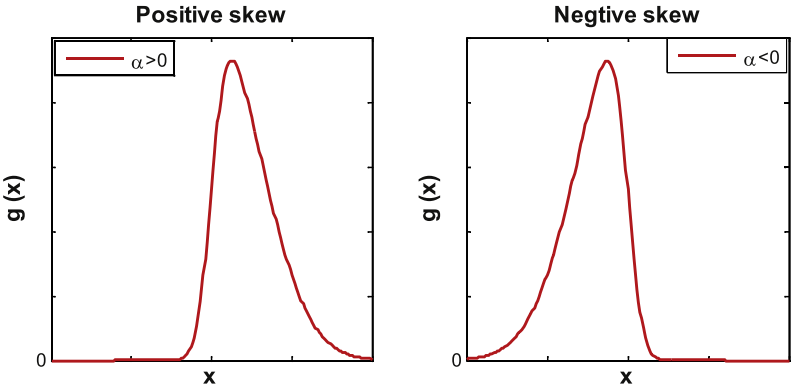

Fig. 8. The skew normal distribution.

of the paper, we will show that summations of the nested probabilities over the corresponding sampling time steps equal to one for each departure time k.

4. Statistical distribution fitting and buffer-time index

4.1. Distribution fitting of dynamic stochastic journey time

After the PMFs of link exit time and journey time are obtained, the problem at hand now is to describe them by appropriate distributions. van Lint et al. (2008) found that the stochastic journey time may not follow the standard normal distribution in which different patterns of skewness can be observed under different traffic conditions. The travel time under the free-flow condition usually follows a normal distribution. On the other hand, under the congested condition or the congestion onset/dissolve process, the link travel time may follow a skewed distribution (van Lint et al., 2008; Kharoufeh and Gautam, 2004). Thus, fitting the PMF to a distribution with skewness should better describe the uncertainty of journey time (or link time). The shape of the journey time distribution will also affect the evaluation of the travel time reliability.

After obtaining the PMF of the path journey time, various random distribution fitting techniques can be applied to obtain the distribution that best fits the estimated PMF. A distribution $T_{rs}(k) = g(\bar{\beta}(k), \sigma_{\beta(k)}, \alpha(k))$ is the distribution of the dynamic journey time at time k, if $g(\bar{\beta}(k), \sigma_{\beta(k)}, \alpha(k))$ best fits the PMF and/or the corresponding CMF with mean $\bar{\beta}(k)$, standard deviation $\sigma_{\beta(k)}$ and shape parameter $\alpha(k)$ which reflects the skewness of the distribution $\beta(k)$. In this paper, the skew normal distribution is used to describe the characteristic of the travel time distribution with the PDF (Azzalini and Capitanio, 1999):

$$g(x) = 2\frac{1}{\sqrt{2\pi}}e^{-\frac{x^2}{2}}\int_{-\infty}^{\alpha x}\frac{1}{\sqrt{2\pi}}e^{-\frac{t^2}{2}}dt,$$

where the distribution is called positive skew, if $\alpha > 0$, that is with a longer right tail and concentrating on the left side; while negative skew, if $\alpha < 0$, that is with a longer left tail and concentrating on the right side (see, e.g. Fig. 8). A direct reason for us to adopt the skew normal distribution is that it generalizes the normal distribution (which is widely utilized in transportation literature and the SCTM framework) to allow for non-zero skewness.[11]

Remark 4.1. Fitting the PMF and CMF to certain distribution is mainly a preparation for travel time reliability analysis. If one only required to calculate the mean, variance and skewness of the distribution, standard technique can be directly applied to the PMF and CMF without fitting the PMF to a particular statistical distribution. For example, the mean travel time $\bar{\beta}(k)$ can be calculated via weighted average algorithm as:

$$\bar{\beta}(k) = \sum_{k'=k_{lb}}^{k'=k_{ub}} P(k'|k)\cdot(k'-k). \tag{11}$$

The confidence interval, e.g. 90% confidence interval bounded by 5th percentile and 95th percentile, can be obtained directly from CMF. Finally, the skewness can be evaluated by:

$$\alpha(k) = \frac{\sum_{k'=k_{lb}}^{k'=k_{ub}} P(k'|k)\cdot\left((k'-k)-\bar{\beta}(k)\right)^3}{\sum_{k'=k_{lb}}^{k'=k_{ub}} P(k'|k)\cdot\left((k'-k)-\bar{\beta}(k)\right)^{3/2}}. \tag{12}$$

[11] The skew normal distribution was found to be a mathematically tractable extension of the normal distribution with the addition of a parameter to regulate skewness that has reasonable flexibility in real data fitting especially for multivariate cases (Azzalini et al., 1999). The skew normal distribution also maintains some convenient formal properties of the normal distribution. In particular, the associated distribution theory of linear and quadratic forms remains largely valid.

4.2. Index of travel time reliability

As previously explained, there are many different definitions for travel time reliability. Different indices are appropriate for different purposes and circumstances. A comprehensive overview of travel time reliability measures can be found in (Lomax et al., 2003; Texas Transportation Institute and Cambridge Systems Inc., 2006; van Lint et al., 2008), here we summarize several measures for travel time reliability in brief for completeness.

- Statistical range methods, which is directly related to the shape of travel time distribution (Bates et al., 2001; Lomax et al., 2003). For instance, Travel Time Window (e.g. mean travel time ± a factor times standard deviation). The underlying "plus" or "minus" operation indicates the possible spread of travel time around the expected value, wherein the distribution of travel time is implicitly assumed to be symmetric. Some other measures that can be categorized into this sort are the Percentage Variation (i.e. the ratio of standard deviation and mean travel time), the Variability Index (the ratio between 95% travel time during peak hours and 95% during off peak). Theoretical (Kharoufeh and Gautam, 2004) and empirical (van Lint et al., 2008) studies have revealed that symmetrical distribution of travel time is valid only under the assumptions that individual vehicles maintain a constant speed and that speeds are symmetric about their means which probably exists only in the case of free-flow conditions.
- Buffer time methods. The buffer time index (BTI) represents the extra time that travelers must add to their average travel time when planning trips to ensure their on-time arrivals (or to have less than X% chance to miss an appointment) (Lomax et al., 2003; Texas Transportation Institute and Cambridge Systems Inc., 2006). The buffer time calculates the minutes of extra time needed to guarantee a statistically minimum number of arrivals within the preferred arrival time at destination. In literature, see e.g. (Lomax et al., 2003; Texas Transportation Institute and Cambridge Systems Inc., 2006), buffer time is expressed as the distance between 90th or 95th percentile travel time and the average travel time. If the 95th percentile travel time is chosen, the buffer time index can then be calculated by Eq. (13):

$$\text{Buffer time index} = \frac{\text{95th Percentile travel time} - \text{Average travel time}}{\text{Average travel time}} \times 100\%. \tag{13}$$

As an extension of BTI, planning time index (PTI) evaluate the ratio of the time needed to ensure on-time arrival (or less than X% chance to miss) to the free-flow travel time:

$$\text{Planning time index} = \frac{\text{95th Percentile travel time}}{\text{Free-flow time}} \times 100\%. \tag{14}$$

- Tardy trip measure defines a threshold to identify an acceptable late arrival time to describe the travel time unreliability using the amount of trips that result in late arrivals, e.g. misery index is defined as the gap between the average travel time of the 20% worst trips and the overall mean travel time (Lomax et al., 2003; Texas Transportation Institute and Cambridge Systems Inc., 2006).
- Probabilistic measures: the probability that a trip would be made within the nominal travel time multiplied by a prescribed factor (Bell, 1999; Yang et al., 2000). The probabilistic measures are often used as measure for travel time unreliability in literature. Probabilistic measures utilize either a threshold for travel time or a predefined time window to distinguish between reliable and unreliable travel times. In this sense, choosing the parameters (e.g. prescribed factor) properly is essential for these probabilistic measures, which renders they are application and context specific.
- Skew-width measures, wherein skewness of travel time is defined as the ratio of the distance between the 90th and 50th percentile travel time to the distance between the 50th and 10th percentile travel time. In general, the larger skewness of travel time means a higher probability for extreme travel times (relative to the mean travel time) to occur.

The main motivation and advantage of the stochastic network framework is its capability to incorporate travel time variability into travelers decisions (Bell and Cassir, 2000, 2002; Bates et al., 2001). Buffer time index and planning time index are the most frequently utilized measures to quantify travel time reliability (Lomax et al., 2003; Texas Transportation Institute and Cambridge Systems Inc., 2006). Obviously, a higher BTI means a greater variance compared with mean travel time but a higher PTI implies a greater travel time budget for on-time arrival. To this end, also for the illustrative purpose the BTI and PTI are adopted as the measures of travel time reliability for the case studies in this paper, where the probability of arriving on-time is set at the 95th percentile which can be translated as "can be late for work 1 day per month without getting into too much trouble" or 95% of travel time observations can be found under this criterion.

5. Empirical studies

This section presents two empirical studies to illustrate and validate the proposed algorithm for evaluation of stochastic dynamic link and route travel time distributions with application to journey time reliability analysis. The first study is tested

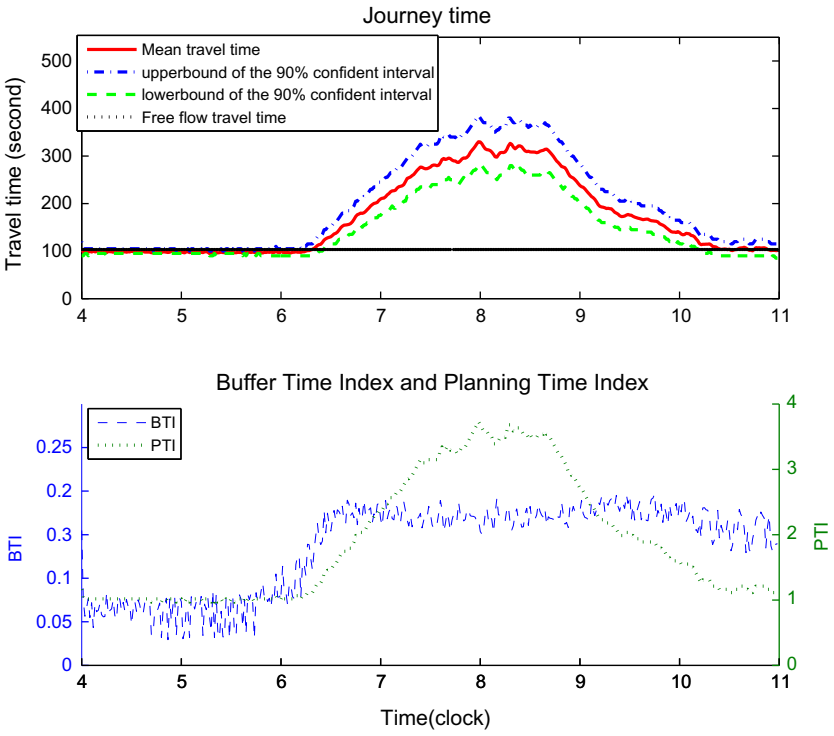

Fig. 9. Journey time distribution and reliability indexes for a freeway segment of I210W.

on a short freeway section of Interstate-210W near Los Angeles while the second case concentrates on a long corridor of Hanshin expressway between Toyonaka and Osaka in Japan. Generally speaking, the first study is a complementary part of the empirical study in Sumalee et al. (2011) wherein historical data of 30 days collected by PeMS is utilized to simulate the effects of both demand and supply uncertainties. The second test intends to illustrate the effects of traffic incidents on journey time distribution and its reliability under different traffic conditions. Robustness of the proposed algorithm against different choices of parameters i, j, ε is also shown in this test. The second case also tries to compare the estimation results considering covariance structure with those obtained under independent assumption.

5.1. A freeway segment of I210-W, California

In this empirical study, we adopt the data from the empirical study in Sumalee et al. (2011) wherein the traffic flow estimation problem was conducted to validate the performance of the SCTM. In this section, we import the flow estimation results obtained in Section 5.3 of Sumalee et al. (2011) to the the proposed algorithm to evaluate the stochastic dynamic travel time and its reliability. Detailed description of the test site, calibration and traffic flow evaluation are given in Sumalee et al. (2011).

Fig. 9 depicts the evaluation of journey time and its reliability indexes. The journey time is about 100 s from 4:00 am–6:00 am. The uncertainty of journey time is small as reflected by the confident interval and the BTI curve. This route is very reliable for this time period as the BTI is below 0.1.[12] Due to the morning peak, the journey time starts to increase smoothly (because of the average effect of the 30 days' data). The variability of journey time also increases with respect to congestion onset, congested traffic and congestion off-set as illustrated by the confident interval and BTI in Fig. 9. However, the journey time can still be considered as reliable as the BTI is around 0.2. This implies that the journey time of this freeway segment is stable with repect to day-to-day (recurrent) demand uncertainty. Although it is not very significant, we can observe that the BTI admits larger values during congestion onset and congestion offset than very congested traffic condition. Similar findings are reported by Higatani et al. (2009) and be "duplicated" in the next empirical study for a long freeway corridor, wherein it

[12] BTI is adopted to quantify travel time reliability in PeMS. A route is considered as reliable for all time periods when the BTI is less than 0.2, moderately reliable when the BTI is between 0.2 and 0.4, and unreliable when the BTI exceeds 0.4.

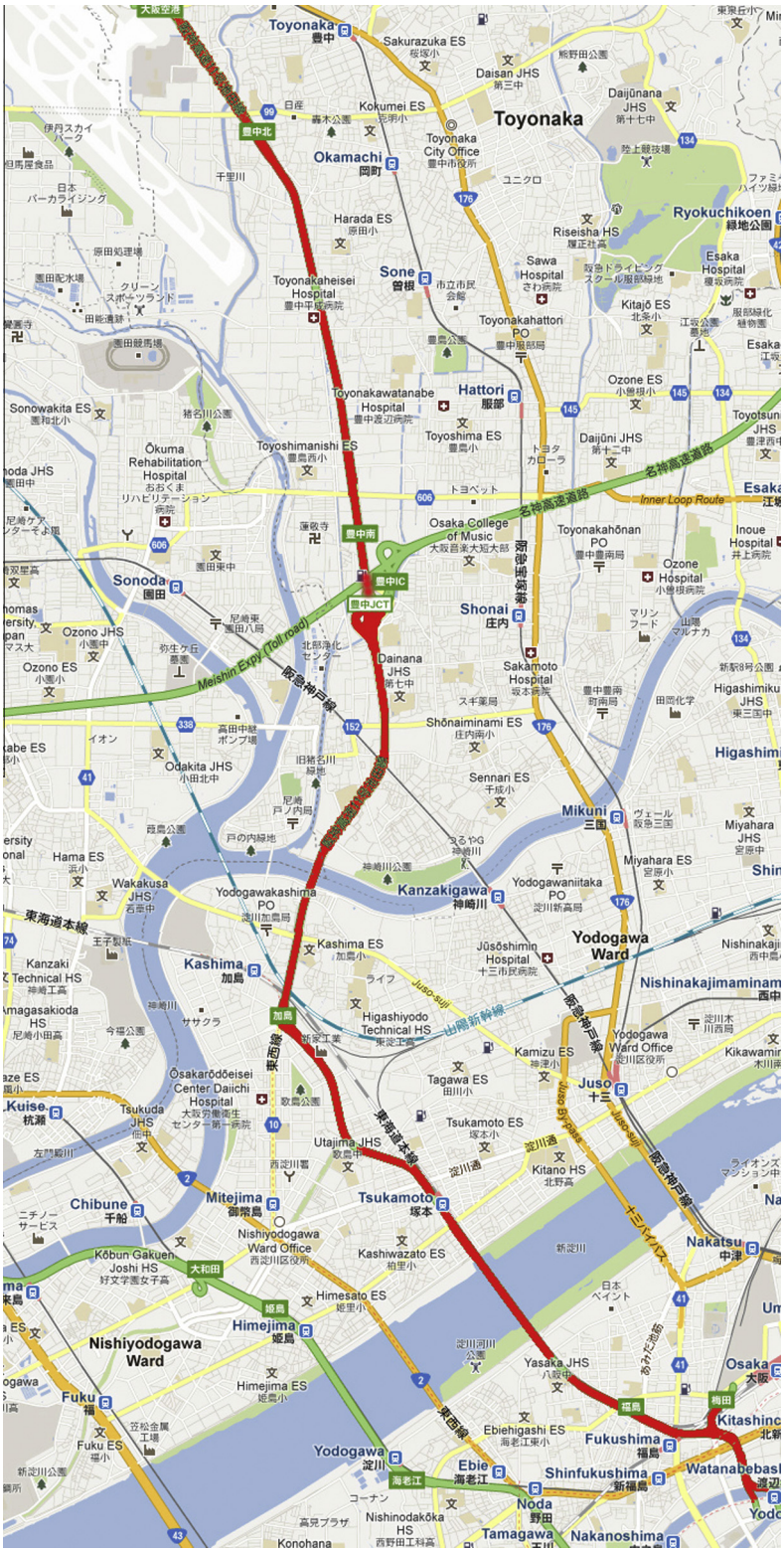

Fig. 10. Map of the test site (*Source:* Google map).

is claimed that peaks of the average travel time do not coincide with those of the buffer time index whereas the tendency of PTI is consistent with that of average travel time as depicted in Fig. 9. Note that the BTI does not decrease to that of the free-flowing

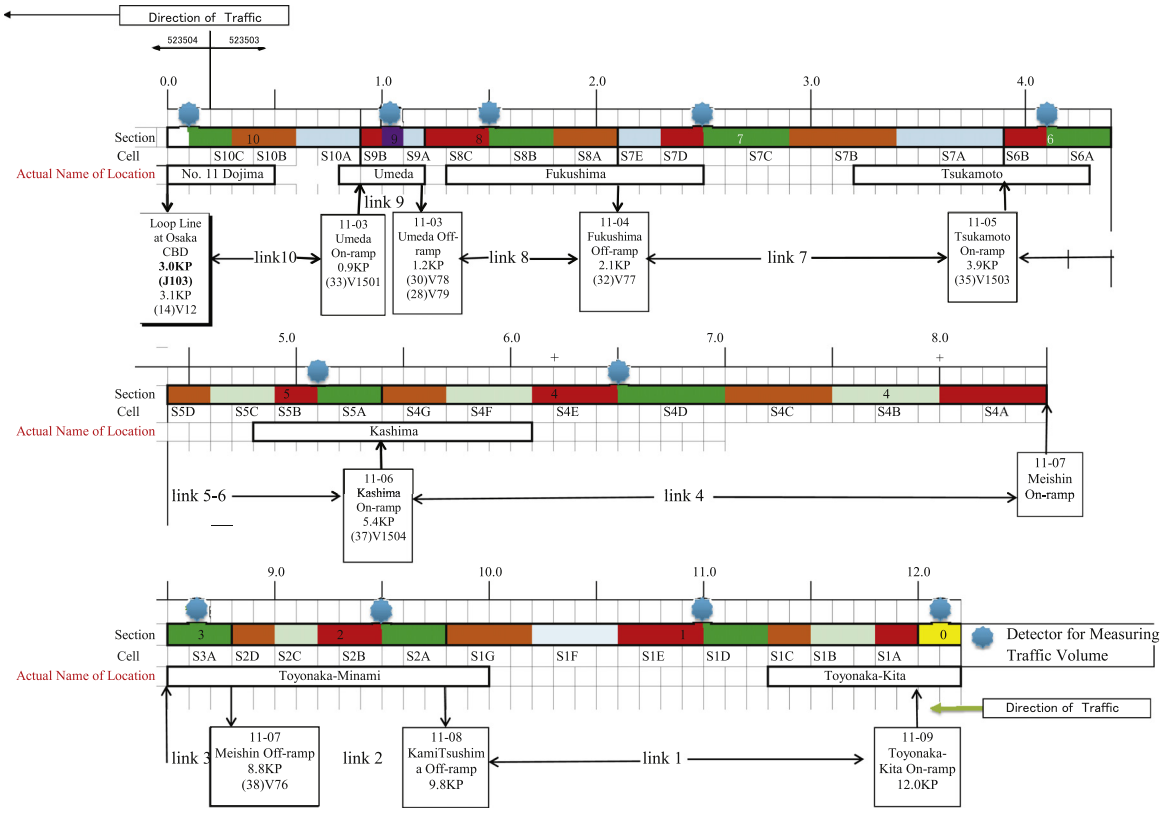

Fig. 11. Segments and links of the corridor.

Table 1
The parameters of fundamental diagrams along the route under normal traffic condition.

Link ID (length/km)	Section ID	$\hat{v}_f$	$\sigma_{\hat{v}_f}$	$\hat{w}_c$	$\sigma_{\hat{w}_c}$	$\hat{\rho}_c$	$\hat{\rho}_J$	$\sigma_{\hat{\rho}_J}$	$\hat{Q}_m$	$\sigma_{\hat{Q}_m}$
Link 1 (2.2)	Section 1	82	6.2	13	5.0	39	279	98	3300	248
Link 2 (1.0)	Section 2	106	16.2	14.5	4.9	28.1	235	78.5	3000	456
Link 3 (0.3)	Section 3	78	9.2	13.6	3.7	44.3	302	76.3	3500	407
Link 4 (3.1)	Section 4	73	6.5	23.8	6.6	54.2	222	50.6	4000	350
Link 5–6 (1.5)	Section 5	78	18.6	22.3	9.9	51	231	100	4000	953
	Section 6	83	7.4	18.8	5.2	48	261	63.3	4000	356
Link 7 (1.8)	Section 7	71	5.2	19.7	6.2	55.7	259	70.6	4000	288
Link 8 (0.9)	Section 8	72	5.1	23.8	4.3	56.6	225	31.0	4000	289
Link 9 (0.3)	Section 9	73	6.5	16.2	5.2	52.0	286	84.0	3800	340
Link 10 (1.0)	Section 10	69	6.3	13.1	2.7	76.8	436.8	64.0	4000	367

stage even though the mean travel time decreases to free-flow time. This is because: on the one hand, the corresponding variance is much larger than that of the free-flowing stage; on the other hand, the mean traffic density is closed to the critical density (as shown in Figs. 25–26 of Sumalee et al. (2011)) which implies that the freeway segment is still in the process of congestion offset. In contrast, the PTI decreases with respect to the mean travel time.

5.2. Ikeda south bound of Hanshin expressway

5.2.1. Description of the test segment and data preparation

This empirical study is conducted on a 12 km segment of No.11 Hanshin Expressway Ikeda corridor from Toyonaka city to the CBD of Osaka as depicted in Fig. 10. This expressway, which includes 10 sections, is composed of 9 links determined by the on-ramps and off-ramps as shown in Fig. 11. Table 1 presents the calibration results of fundamental diagrams based on

Table 2
Assignment of cells and segments for SCTM.

Link ID	Section ID	Cell ID and length (km)	SCTM segment ID
Link 1	Section 1	Cell S1A (0.2)*	Segment S1A–S1D
		Cell S1B (0.3)	
		Cell S1C (0.2)	
		Cell S1D (0.3)*	
		Cell S1E (0.4)*	Segment S1E–S2A
		Cell S1F (0.4)	
		Cell S1G (0.4)	
Link 2	Section 2	Cell S2A (0.3)*	
		Cell S2B (0.3)*	Segment S2B–S3
		Cell S2C (0.2)	
		Cell S2D (0.2)	
Link 3	Section 3	Cell S3 (0.3)*	
Link 4	Section 4	Cell S4A (0.5)*	Segment S4A–S4D
		Cell S4B (0.5)	
		Cell S4C (0.5)	
		Cell S4D (0.5)*	
		Cell S4E (0.4)*	Segment S4E–S5A
		Cell S4F (0.4)	
		Cell S4G (0.3)	
Link 5–6	Section 5	Cell S5A (0.3)*	
		Cell S5B (0.2)*	Segment S5B–S6A
		Cell S5C (0.3)	
		Cell S5D (0.2)	
	Section 6	Cell S6A (0.3)*	
		Cell S6B (0.2)*	Segment S6B–S7C
Link 7	Section 7	Cell S7A (0.5)	
		Cell S7B (0.5)	
		Cell S7C (0.4)*	
		Cell S7D (0.2)*	Segment S7D–S8B
		Cell S7E (0.2)	
Link 8	Section 8	Cell S8A (0.3)	
		Cell S8B (0.3)*	
		Cell S8C (0.2)*	Segment S8C–S9A
Link 9	Section 9	Cell S9A (0.2)*	
		Cell S9B (0.2)*	Segment S9B–S10C
Link 10	Section 10	Cell S10A (0.3)	
		Cell S10B (0.3)	
		Cell S10C (0.2)*	

Table 3
Incident record of the main road between 7:00 and 21:00 on Monday.

Incident ID	Incident occurrence date	Incident occurrence time	Incident ending date	Incident ending time	Cause	Severity	Location	Cells involved
1898	2008/5/12	7:16:00	2008/5/12	7:28:00	Jam		4.0–5. 0	Cell 5B–6B
1599	2008/5/12	8:30:00	2008/5/12	10:35:00	Traffic accident	One lane closure	0.7–0.9	Cell 10A
1415	2008/5/12	10:02:00	2008/5/12	10:14:00	Obstacle dropped from veh.	One lane closure	0.2	Cell 10C
1910	2008/5/12	8:43:00	2008/5/12	10:36:00	Jam		3.0–3.0	
1909	2008/5/12	8:38:00	2008/5/12	10:35:00	Jam		0.7–0. 9	Cell 10A
1417	2008/5/12	10:41:00	2008/5/12	10:50:00	Mulfunction of veh.	One lane closure	1.0–3.0	Cell 7B–Cell 9B

the historical data under the normal traffic condition (i.e. no incident), which is provided by detectors equipped within each section. The historical data, which will be used in simulation, includes flow and speed, which is provided by all the 11 detectors from 0:00 am of May 11 (Sunday), 2008 to 23:55 pm of May 17 (Saturday), 2008 with a resolution of 5 min.[13] A simulation time increment of 10 s is chosen for this study. Table 2 depicts the assignment of cells along the whole expressway

[13] This data set is indeed not sufficient enough to produce accurate calibration and subsequent simulation results. However, insufficient data and lack of incident records (or inaccurate records) are very common in practice. One of the purposes of this empirical study is to demonstrate that the SCTM and the proposed algorithm can produce satisfactory results even under insufficient data and lack of incident records.

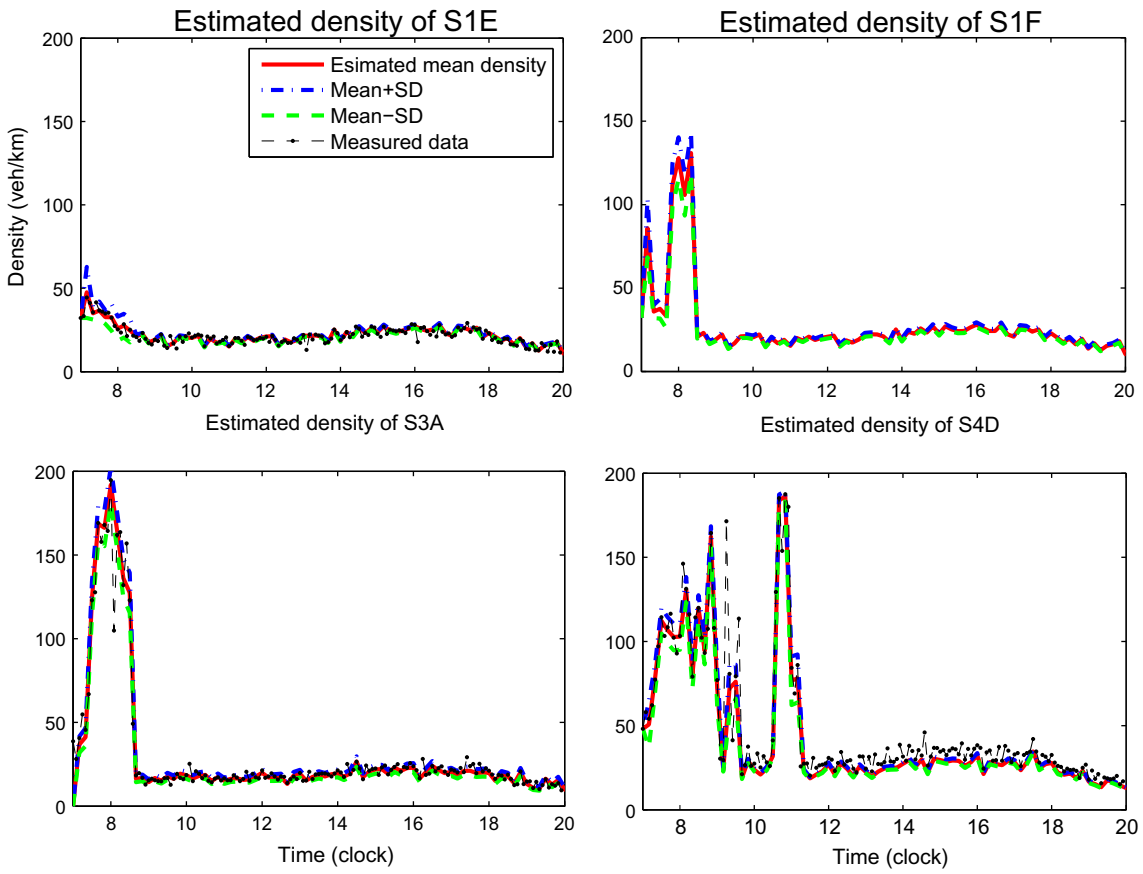

Fig. 12. Measured and estimated density with 68% confidence interval.

corridor, where the 38 cells mentioned in the table constitute the 10 SCTM segments and the cells with superscript "∗" are those equipped with detectors.

The objective of this empirical study is to simulate the effects of traffic incidents on the dynamic journey time and traffic states, e.g. how would different incident locations, time of occurrence and duration generate different kinds of traffic jams. Table 3 gives a demonstration of incident record which indicates 3 accidents and 3 jams occurred during 7:00 am–21:00 pm on May 12, 2008 on the main road. Jam 1898 during 7:16 am–7:28 am started from Link 5 and Link 6 was not caused by accident. Jam 1909 and Jam 1910 during 8:38 am–10:35 am on Link 10 and its upstream segments were induced by Incident 1599 and Incident 1419 during 8:30 am–10:35 am on Link10, while Incident 1417 did not lead to any congestion. Note that the information on the jams are not complete, e.g. the spillback effects of congestion are not recorded in the database.

5.2.2. Traffic states under incident scenarios

Figs. 12–16 present the simulation results generated by the SCTM and the proposed stochastic dynamic travel time algorithm based on the parameters listed in Table 1, detected boundary conditions, and the incident records. The fundamental diagram parameters are adjusted in accordance with the lane closure conditions under traffic accidents.

As shown in Fig. 12, cells S1A–S1E maintain free flowing condition throughout the whole simulation period.[14] This implies that this segment was not influenced by any spillback effect of the congestion caused by incidents or other jams. However, from cell S1F and onward (from upstream to downstream), all the downstream links suffered from congestion induced by the spillback effect caused by Jam 1898 originated from cells S5B–S6B (i.e. post kilometer 4–5 km in the incident record) at 7:16 am. The congestion wave-front spent about 25 min to reach cell S1F. We may roughly deduce the average speed of this backward wave to be about 16 km/h, which is close to the average of the calibrated mean values (about 17 km/h). Jam 1909 and Jam 1910 were induced by Incident 1599 at cell S10A. The congestion wave propagated to upstream until it reached cell S4D. During this spillback process, the congestion wave caused by Jam 1909 and Jam 1910 merged with that caused by Jam 1898 at S7A. From the

[14] Indeed, cells S1B, S1C and S1D are also free flowing which are not depicted in the figure. We do not present the simulation results for all cells due to limited space. Simulation results of cells equipped with detectors and those related to incident induced congestion are demonstrated for the purpose of comparison.

simulation results, we can observe that both traffic density and its variance are propagating backward to the upstream cells under congested traffic conditions. The sudden increase of traffic density of cell S10C around 10:10 am reflects the effect of Incident 1415. However, no obvious congestion was caused by this incident as it did not cause dense traffic on cell S10C and its adjacent cells. Similarly, Incident 1417 did not lead to any significant disturbance to the traffic flow. These reflect that the effect of an incident on traffic flow is not significant if its time of occurrence is inside the off-peak hours. On the other hand, congestion wave would traverse fast during peak hours which in turn yields long queues induced by traffic incidents. This symbiotic relationship between congestion and traffic incidents has been reported in traffic incident literature (Özbay and Kachroo, 1999). To be precise, congested traffic condition is one of the main reasons for traffic accidents. Incidents on freeways interrupt traffic flows unexpectedly which cause "unusual" bottlenecks and secondary accidents. Those accidents cause more congestion, which in turn, causes more accidents.

The estimated traffic densities against the corresponding detected ones presented in Figs. 12 and 13 confirm that the SCTM performs well in stochastic traffic state estimation even under incidental and congested traffic scenarios. Moreover, the model is also able to capture congestion formation, spillback and dissolve. These stochastic densities are suitable for the applications of dynamic stochastic journey time and the subsequent journey time reliability analysis.

5.2.3. Journey time estimation and its reliability analysis

Given the estimated stochastic dynamic cell densities, we are ready to estimate dynamic link travel time distributions of the 9 links by the proposed PMF based algorithm. To fulfil our purpose of investigating traffic incident effects on dynamic journey distribution and its reliability analysis, we here present only the results closely related. Table 4 presents the MAPE (Mean Absolute Percentage Error) of estimated journey time compared with the available measured travel times. The results confirm a satisfactory performance of the proposed method. Table 5 presents the MAPE of journey time for Path 1 with different pairs of ε and i, j. The table illustrates that the accuracy of journey time generally remains almost the same. This implies that the proposed method is not sensitive to the choice of these parameters. We also calculate the dynamic travel time distribution by incorporating the covariance structure of traffic flow according to the method depicted in Appendix A.1. The MAPE obtained is 9.9%. Compared with that obtained by the independent assumption, which is 9.93%, the difference is not significant.

Since the journey time over the whole corridor (from link 1 to link 10) is not directly provided by the database, Fig. 14 depicts the journey time estimation results and the reliability indexes. At the beginning of the simulation horizon, the jour-

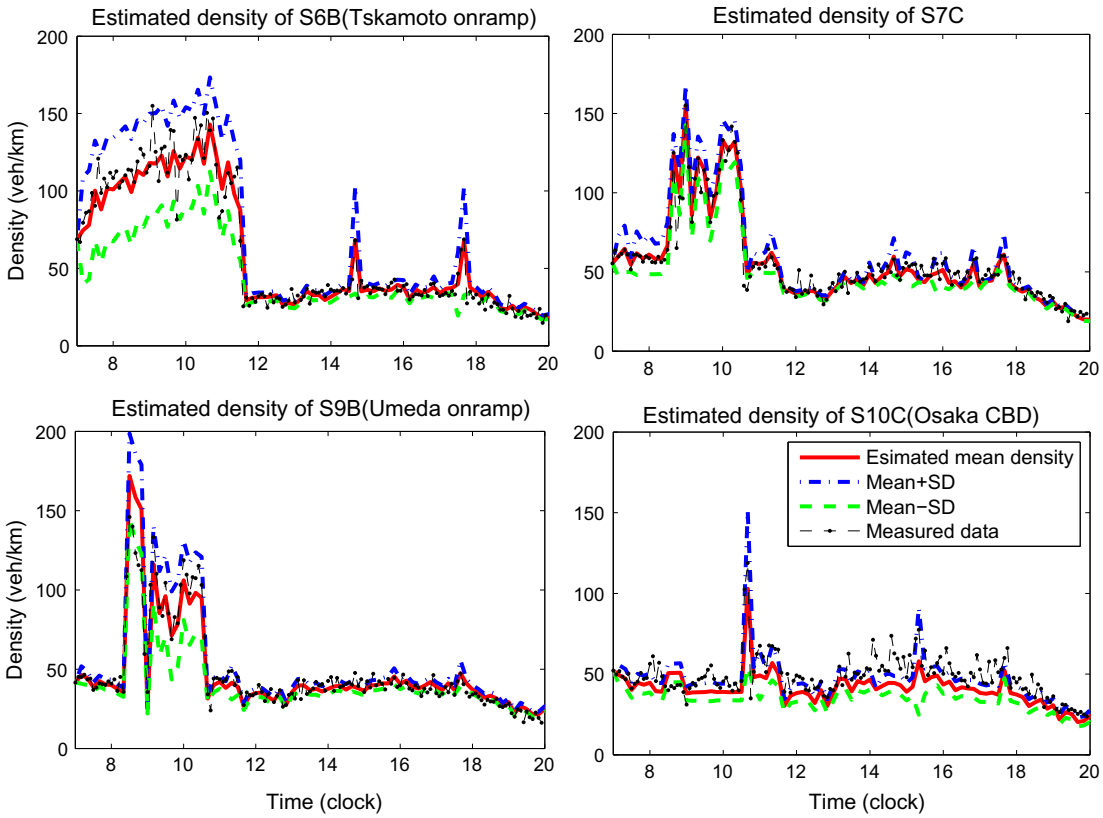

Fig. 13. Measured and estimated density with 68% confidence interval.

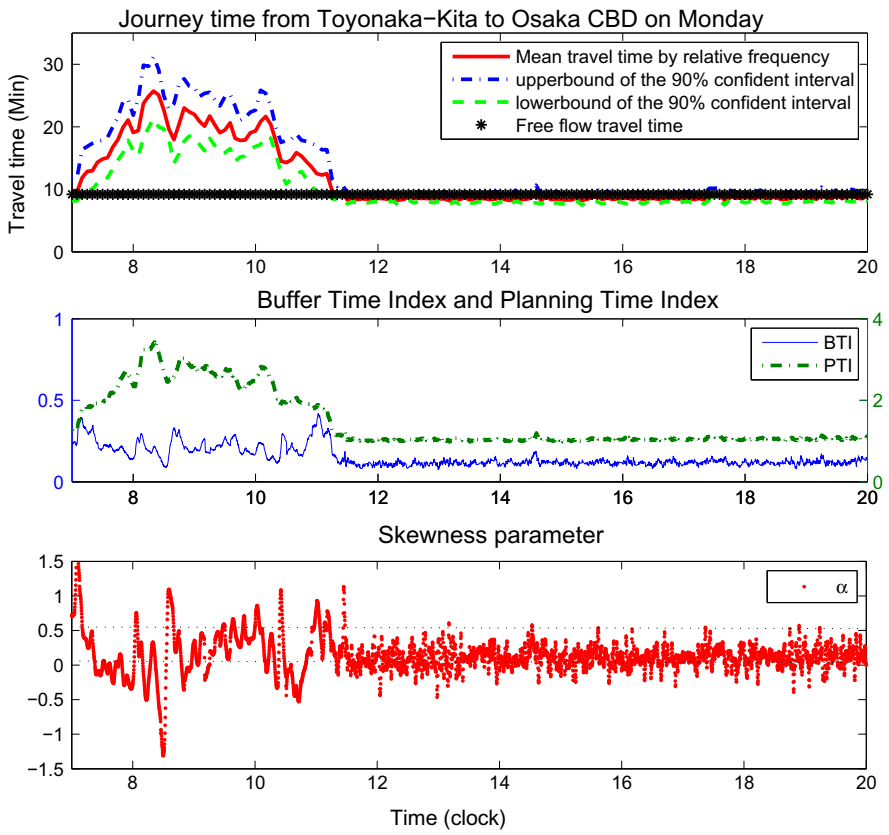

Fig. 14. Journey time distribution and reliability indexes.

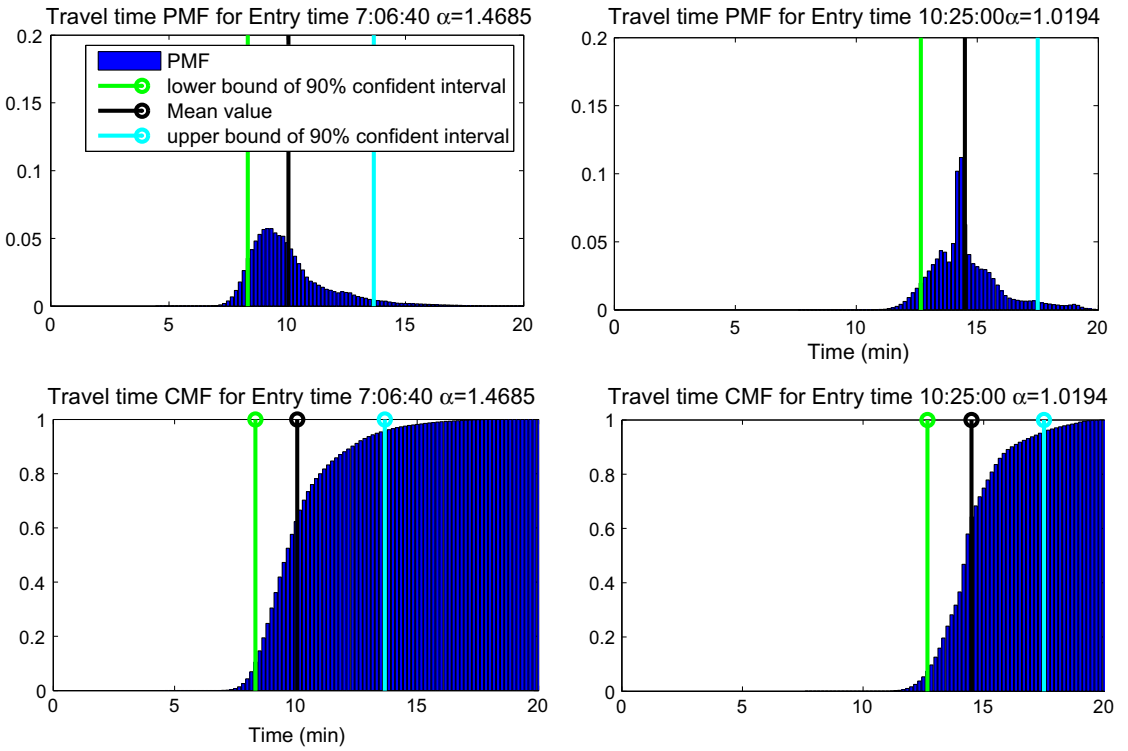

Fig. 15. Positively skew journey time distribution.

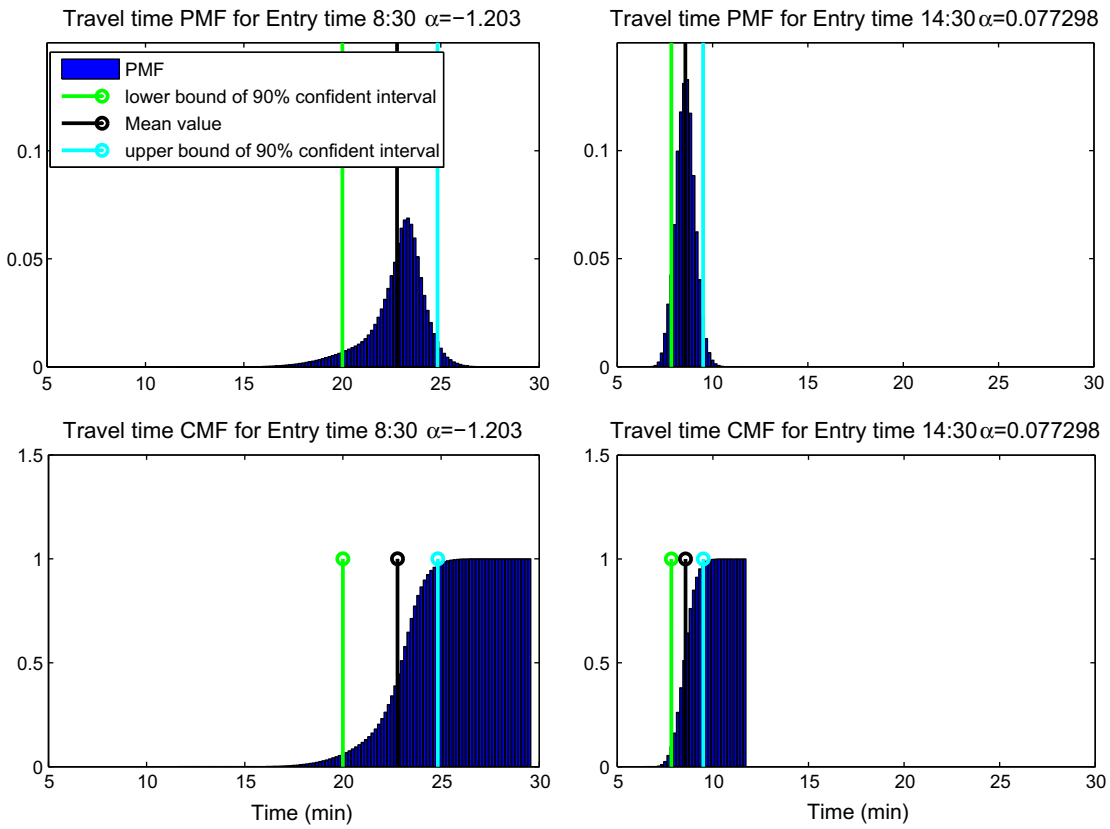

Fig. 16. Negatively skew journey time distribution.

Table 4
MAPE of the estimated journey time.

Journey	Path 1 (from link 1 to 2)	Path 2 (from link 1 to 7)	Path 3 (from link 1 to 8)
MAPE	9.93%	9.75%	9.78%

Table 5
MAPE of the estimated journey time of Path 1 with different parameter sets.

MAPE			
i, j	ε		
	0.5 (%)	1 (%)	2 (%)
$[-\sigma,\sigma]$	10.5	10.5	10.7
$[-3\sigma,3\sigma]$	9.93	9.93	9.94
$[-4\sigma,4\sigma]$	9.93	9.93	9.95

ney time was about 10 min. However, the journey time remained at such a small value only for about 5 min and started to increase sharply since 7:05 am due to Jam 1898. This congestion period increased the journey time to 25 min, which is about 3 times of the free-flow time. At about 8:00 am, the journey time reduced a bit due to the dispersion of Jam 1898, while it increased again due to Jam 1909 and Jam 1910 started from about 8:30 am. Finally, the journey time reduced to free flow time after all these congestions were dissolved. Fig. 14 also presents the BTI and PTI of the journey time in the second figure. The unreliable periods concentrate during 7:05 am–11:30 am due to the jams and incidents. The peaks of travel time reliability index appear at three times: (1) the congestion onset progress around 7:12 am caused by Jam 1898; (2) the intersec-

tion of congestion dissolve of Jam 1898 and congestion onset of Jams 1909/1910 around 8:30 am; (3) the final congestion dissolve around 11:15 am. The buffer time index shows that the route travel time was quite stable except for the congestion parts caused by peak-hour demand and incidents which is consistent with the findings in Higatani et al. (2009). In Higatani et al. (2009), the authors found also that peaks of the average travel time do not coincide with those of the buffer time index. Indeed, the BTI would have larger value if the corresponding distribution is more variable. Moreover, under very congested traffic condition (which is a steady state), the variability of travel time is smaller than those under congestion onset and offset (which are transient states) whereas the mean travel time under congested traffic condition is larger than those under congestion onset and offset. In Higatani et al. (2009), it is claimed that the peak of buffer time index comes after the peak of the average travel time for this expressway corridor. This coincides with our finding that the peaks of buffer time index appear during congestion on-set and off-set, whereas the tendency of PTI is consistent with that of average travel time.

From Fig. 14, it can be observed that the gaps between the mean travel time with the upper bound of 90% confidence interval and that with the lower bound are not equivalent. This implies that travel time is skewed distributed. van Lint et al. (2008) concluded the characteristics of skewness during the different periods of congestion:

1. Congestion onset: the mean travel times are increasing, and the distribution is positively skew.
2. Congestion dissolve: the mean travel times are decreasing, and the distribution is positively skew.
3. Congestion: the mean travel times are high, while the travel time distribution is wide and either symmetric or slightly negatively skew.
4. Free flow: the mean travel times are low, and the travel time distribution is narrow and either symmetric or slightly negatively skew.

The above conclusions were based on the analysis of statistics. However, in this research, similar results can also be observed from the simulation results of this empirical study, such as the shape parameters of the stochastic travel time as depicted in Fig. 14. Generally, the journey times are positively skew during the congestion onset and congestion dissolve periods (referring to the traffic density). During the stationary stages of congestion (during 7:30 am–8:15 am by referring to traffic density), mainly symmetric and (slightly) negatively skew can be observed. Another congestion onset starts at around 8:20 am which yields another period of positively skew distribution of travel time. Similar analysis can be applied to congestions caused by other incidents. After 11:30 am, the journey times are approximately symmetric normally distributed. In order to illustrate the characteristics of the skewness of journey time, Figs. 15 and 16 depict the PMFs and corresponding shape parameter to assist the comprehension. The positively skew distributions in Fig. 15 confirm Conclusion (1) and (2) by presenting the PMFs of the journey times during congestion onset progress at 7:06:40 am and congestion dissolve progress at 10:25:00 am. Fig. 16 confirms Conclusion (3) and (4) by the negatively skew distributions at 8:30 am under congested condition and the symmetric distribution at 14:30 pm under free flowing condition respectively.

6. Conclusions

This paper proposed an algorithm to estimate/predict dynamic stochastic journey time distribution and to assess the dynamic journey time reliability based on the stochastic cell transmission model (Sumalee et al., 2011). Stochastic cumulative link inflow and outflow profiles were generated the SCTM. The algorithm for calculating the probability mass function (PMF) of the stochastic dynamic journey time was proposed by devising the sampling process of the cumulative flows for each entry time interval. The journey time was then estimated by extending the nested delay operator to the stochastic case based on the conditional probability. The paper also proposed a method to fit the estimated PMF of the journey time to a class of skew normal distribution to determine the skewness of the journey time distribution.

The model and the algorithm were tested with the two empirical case studies, and the results showed that the algorithm is applicable both for the prediction based on the historical data and the estimation given the incident record. The skewness of the journey time distribution proposed in the first empirical study was generally consistent with the statistical results reported by van Lint et al. (2008). The second empirical study on an expressway between Toyanaka-kita and Osaka CBD illustrated that the model and the algorithm are capable of simulating traffic conditions caused by the jams and incidents. Motivated by the current results, our future work will be built on the SCTM and the proposed journey time estimation algorithm to detect incident/abnormal traffic states on real-time basis. On the other hand, the proposed methods have potential applications in stochastic dynamic traffic assignment studies. In the deterministic dynamic traffic assignment framework, four key components are required: (i) models of link and path delays; (ii) flow dynamics; (iii) flow propagation constraints; and (iv) a route/departure-time choice model. All these components are either missing from the literature on stochastic dynamic traffic assignment or not very well defined. The SCTM offers an approach to describe components (ii) and (iii). The link and route travel time calculation methods developed in this paper offer the first component.

Acknowledgements

This research is sponsored by the Research Fund projects (PolyU 5271/08E and PolyU 5250/11E) of the Hong Kong Research Grant Council. The author also would like to thank the Freeway Performance Measurement (PeMS) Project and the Hanshin Expressway for providing the data in the empirical studies.

Appendix A

Key notations	
l_m	link m, $m = 1, 2, \ldots, Nl$
p	path p
S_j	segment j, $j = 1, 2, \ldots, Ns$
s	operational mode of the SCTM, $s = FF, CC, CF, FC1, FC2$
t	discrete time interval
$q_{in}^{l_m}(t)$	inflow rate of link l_m at time t
$q_{out}^{l_m}(t)$	outflow rate of link l_m at time t
$C_{in}^{l_m}(t)$	cumulative inflow of link l_m up to time t
$C_{out}^{l_m}(t)$	cumulative outflow of link l_m up to time t
$\tau_{l_m}(t)$	exit time from link l_m for vehicles entering link l_m at time t
$\beta_{l_m}(t)$	link travel time of l_m for vehicles entering link l_m at time t
$\eta_p(t)$	journey time of path p for vehicles entering the origin at time t
$\tilde{\rho}_u(k)$	measured density at the upstream boundary of a segment at time step k
$\tilde{\rho}_d(k)$	measured density at the downstream boundary of a segment at time step k
$\tilde{q}_u(k)$	measured inflow rate at the upstream boundary of a segment at time step k
$q_{in}^{l}(k)$	inflow rate of link l at time step k
$q_{out}^{l}(k)$	outflow rate of link l at time step$k$
$\overline{C}_{in}^{l_m}(k)$	mean of the cumulative inflow of link l_m up to time step$k$
$\sigma_{C_{in}^{l_m}}(k)$	standard deviation of the cumulative inflow of link l_m up to time step$k$
$[k_{lb}, k_{ub}]$	sampling time interval for link exit time for vehicles entering the link at time step k
$P'_{k'\|k}$	likelihood of the exit time to be k' for vehicles entering the link at time step k
$P_{k'\|k}$	relative frequency of the exit time to be k' for vehicles entering the link at time step k
$\rho_i^{l_m}(k)$	estimated traffic density of cell i on link l_m at time step k
$P_{m,nest}(k^m\|k)$	relative frequency of k^m to be the exit time step from link l_m for vehicles entering the origin of the path at time step k

A.1. Variance of the matching error

To calculate the variance of the matching error, it is convenient for us to express it in a vector form so as to make use of the property of multivariate normal distribution (Gut, 2009; Härdle and Simar, 2007; Johnson and Wichern, 2007). Let

$$a = \left(-s_1^{l_m}, -s_2^{l_m}, \ldots, -s_{NC_{l_m}}^{l_m}, \Delta t, \ldots, \Delta t\right)^T \in R^{\ell_1},$$

and

$$\mathcal{Q} = \left(\rho_1^{l_m}(k), \rho_2^{l_m}(k), \ldots, \rho_{NC_{l_m}}^{l_m}(k), q_{out}^{l_m}(k+1), \ldots, q_{out}^{l_m}(k')\right)^T.$$

The matching error can then be written as $e_k(k') = a^T\mathcal{Q}$. By assumption, $\mathcal{Q}$ has a multivariate normal distribution. Then, $e_k(k')$ is a normally distributed random variable as every linear combination of normally distributed variables is normally distributed (Gut, 2009; Härdle and Simar, 2007; Johnson and Wichern, 2007). The variance of the matching error is now

$$Var(e_k(k')) = Var(a^T\mathcal{Q}) = a^T Var(\mathcal{Q})a, \tag{15}$$

while the covariance matrix $Var(\mathcal{Q})$ can be obtained from the SCTM. For the special case, where the components of $\mathcal{Q}$ are assumed to be independent, $Var(\mathcal{Q})$ is a diagonal matrix which is denoted as Γ_d. By this observation, we may have more interesting results by exploring the relation between the independent case and the dependent case. To begin with, we first introduce the following lemma, which states that we can always find a linear transformation, e.g. Mahalanobis transformation, to transfer a vector of multivariate normal distribution with dependent components into a random vector with independent (standard) normal random variables (Gut, 2009; Härdle and Simar, 2007; Johnson and Wichern, 2007):

Lemma A.1. *For a random vector $\mathcal{Q} \sim N(\mu, \Lambda)$ has a multivariate normal distribution, we have:*

- *There exists a random ℓ_2-vector Z, whose components are independent standard normal random variables, a ℓ_1-vector μ, and a $\ell_1 \times \ell_2$ matrix A, such that $\mathcal{Q} = AZ + \mu$. The covariance matrix of $\mathcal{Q}$ is then given by $\Gamma = AA^T$ with rank$\Gamma = \ell_2$.*

- *Let $H = C^T \mathcal{Q}$, where the orthogonal matrix C is such that $C^T \Lambda C = D$. Then $H \sim N(C^T \mu, D)$. Moreover, the components of H are independent and Var $Y_k = \lambda_k$, k = 1,2,…, ℓ_1, where $\lambda_1, \lambda_1, \ldots, \lambda_{\ell_1}$ are the eigenvalues of Λ.*
- *For the Mahalanobis transformation $Y = \Lambda^{-1/2}(\mathcal{Q} - \mu)$, we have $Y \sim N(0, \mathcal{I})$, i.e., the components of Y are independent standard normal random variables.*

By this lemma, we can always find some invertible linear transformation (i.e. isomorphism), such that the original correlated random vector can be transferred to an independent one. Also note that the variance of $e_k(k')$ with correlated components of $\mathcal{Q}$, say $Var_1(e_k(k'))$, is a linear functions of that with independent components of $\mathcal{Q}$, say $Var_2(e_k(k'))$, i.e. $Var_1(e_k(k')) = b_{k,k'} Var_2(e_k(k'))$, where $b_{k,k'}$ is certain constant. Thus, the likelihood measure given by Eq. (4) may be changed. However, the relative frequency given by Eq. (8) may not change significantly as shown in the empirical study. The idea of coordinate transformation is commonly utilized in statistics and signal processing theory, e.g. the unscented Kalman filter.

A.2. Properties of the lower and upper bounds and the choice of i, j in Eq. (7)

In the definition of the lower and upper bounds of the sampling time interval as given by Eq. (7), parameters i, j, which can be selected as small positive integers (or non-integers), are added as another degree of freedom to adjust the sampling time interval. Roughly speaking, i, j can be adjusted such that there is no overlapping between the two curves $\overline{C}^{l_m}_{in}(k) - i\sigma_{C^{l_m}_{in}}(k)$ and $\overline{C}^{l_m}_{out}(k') + j\sigma_{C^{l_m}_{out}}(k)$, which can be easily achieved by choosing small enough i, j. In this appendix, we give some insights to the choice of i, j. Foremost among these is the monotonicity of the functions

$$J_1(k') = \left(\overline{C}^{l_m}_{in}(k) - i\sigma_{C^{l_m}_{in}}(k)\right) - \left(\overline{C}^{l_m}_{out}(k') + j\sigma_{C^{l_m}_{out}}(k')\right),$$
$$J_2(k') = \left(\overline{C}^{l_m}_{in}(k) + i\sigma_{C^{l_m}_{in}}(k)\right) - \left(\overline{C}^{l_m}_{out}(k') - j\sigma_{C^{l_m}_{out}}(k')\right),$$

with respect to the exit time index k' given the entry time k. Given k, the terms $\left(\overline{C}^{l_m}_{in}(k) - i\sigma_{C^{l_m}_{in}}(k)\right)$ and $\left(\overline{C}^{l_m}_{in}(k) + i\sigma_{C^{l_m}_{in}}(k)\right)$ are known constants. The monotonicity of $J_1(k')$ is obvious since $\left(\overline{C}^{l_m}_{out}(k') + j\sigma_{C^{l_m}_{out}}(k')\right)$ is monotone increasing with respect to the exit time index k'. The monotonicity of $J_2(k')$ can be achieved by choosing j properly. To see this, let us express $C^{l_m}_{out}(k'+1) = C^{l_m}_{out}(k') + q^{l_m}_{out}(k'+1)$ by definition, where $q^{l_m}_{out}(k'+1)$ is the outflow of link l_m during $[k', k'+1)\ \Delta t$.

$$\begin{aligned} J_2(k'+1) - J_2(k') &= -\left(\overline{C}^{l_m}_{out}(k'+1) - j\sigma_{C^{l_m}_{out}}(k'+1)\right) + \left(\overline{C}^{l_m}_{out}(k') - j\sigma_{C^{l_m}_{out}}(k')\right), \\ &= -\left(\bar{q}^{l_m}_{out}(k'+1) - j\left(\sigma_{C^{l_m}_{out}}(k'+1) - \sigma_{C^{l_m}_{out}}(k')\right)\right). \end{aligned}$$

By definition, we have $\sigma_{C^{l_m}_{out}}(k'+1) = \sqrt{\left(\sigma_{C^{l_m}_{out}}(k')\right)^2 + \left(\sigma_{q^{l_m}_{out}}(k'+1)\right)^2}$. Furthermore, by elementary inequality we have the following relation

$$\sigma_{C^{l_m}_{out}}(k') + \sigma_{q^{l_m}_{out}}(k'+1) = \sqrt{\left(\sigma_{C^{l_m}_{out}}(k') + \sigma_{q^{l_m}_{out}}(k'+1)\right)^2} \geqslant \sqrt{\left(\sigma_{C^{l_m}_{out}}(k')\right)^2 + \left(\sigma_{q^{l_m}_{out}}(k'+1)\right)^2}.$$

The above relationship implies that

$$\sigma_{C^{l_m}_{out}}(k'+1) - \sigma_{C^{l_m}_{out}}(k') \leqslant \sigma_{q^{l_m}_{out}}(k'+1).$$

It is obvious that

$$J_2(k'+1) - J_2(k') \leqslant -\left(\bar{q}^{l_m}_{out}(k'+1) - j\sigma_{q^{l_m}_{out}}(k'+1)\right).$$

The parameter j can be chosen such that $\bar{q}^{l_m}_{out}(k'+1) - j\sigma_{q^{l_m}_{out}}(k'+1) \geqslant 0$ to render the function $J_2(k')$ be a monotone function of k' given an entry time k. However, one may prefer to use fixed j rather than changing the value of j with respect to different traffic condition. In this case, we may adopt the following modification

$$\max\left\{\bar{q}^{l_m}_{out}(k'+1) - j\sigma_{q^{l_m}_{out}}(k'+1), 0\right\},$$

to enforce the monotonicity of envelop curves (thus do not admit oscillations) defined by the lower and upper bounds.

A.3. Summations of the nested probabilities

In this appendix, we will show that summations of the nested probabilities over the corresponding sampling time steps are equal to one for each departure time k. The proof is established by mathematical induction in terms of link sequential order. For the first link l_1 of a route and a given departure time k, we have that

$$\sum_{\tau^1=k_{lb}^{l_1}}^{k_{ub}^{l_1}} P_{1,nest}(\tau^1|k) = \sum_{\tau^1=k_{lb}^{l_1}}^{k_{ub}^{l_1}} P_1(\tau^1|k) = \sum_{k'=k_{lb}^{l_1}}^{k_{ub}^{l_1}} P_{k'|k} = \sum_{k'=k_{lb}^{l_1}}^{k_{ub}^{l_1}} \frac{P'_{k'|k}}{\sum_{k_{lb}^{l_1}}^{k_{ub}^{l_1}} P'_{k'|k}} = 1. \tag{16}$$

Next, we will show that the nested probability of link l_2 over the corresponding sampling time steps equals to one for the departure time k.

$$\sum_{\tau^2=\left(k_{lb}^{l_1}\right)_{lb}^{l_2}}^{\left(k_{ub}^{l_1}\right)_{ub}^{l_2}} P_{2,nest}(\tau^2|k) = \sum_{\tau^2=\left(k_{lb}^{l_1}\right)_{lb}^{l_2}}^{\left(k_{ub}^{l_1}\right)_{ub}^{l_2}} \sum_{\tau^1=k_{lb}^{l_1}}^{k_{ub}^{l_1}} P_2(\tau^2|\tau^1) P_{1,nest}(\tau^1|k).$$

Now, we interchange the order of summation so that

$$\sum_{\tau^2=\left(k_{lb}^{l_1}\right)_{lb}^{l_2}}^{\left(k_{ub}^{l_1}\right)_{ub}^{l_2}} P_{2,nest}(\tau^2|k) = \sum_{\tau^1=k_{lb}^{l_1}}^{k_{ub}^{l_1}} \left(\sum_{\tau^2=\left(k_{lb}^{l_1}\right)_{lb}^{l_2}}^{\left(k_{ub}^{l_1}\right)_{ub}^{l_2}} P_2(\tau^2|\tau^1) \right) P_{1,nest}(\tau^1|k) = \sum_{\tau^1=k_{lb}^{l_1}}^{k_{ub}^{l_1}} P_{1,nest}(\tau^1|k) = 1. \tag{17}$$

Now we assume this is hold for link l_m on the route, that is

$$\sum_{\tau^m=\left(\left(k_{lb}^{l_1}\right)\cdots\right)_{lb}^{l_m}}^{\left(\left(k_{ub}^{l_1}\right)\cdots\right)_{ub}^{l_m}} P_{m,nest}(\tau^m|k) = 1. \tag{18}$$

Then for link l_{m+1}, we have

$$\sum_{\tau^{m+1}=\left(\left(k_{lb}^{l_1}\right)\cdots\right)_{lb}^{l_{m+1}}}^{\left(\left(k_{ub}^{l_1}\right)\cdots\right)_{ub}^{l_{m+1}}} P_{m+1,nest}(\tau^{m+1}|k) = \sum_{\tau^{m+1}=\left(\left(k_{lb}^{l_1}\right)\cdots\right)_{lb}^{l_{m+1}}}^{\left(\left(k_{ub}^{l_1}\right)\cdots\right)_{ub}^{l_{m+1}}} \sum_{\tau^m=\left(\left(k_{lb}^{l_1}\right)\cdots\right)_{lb}^{l_m}}^{\left(\left(k_{ub}^{l_1}\right)\cdots\right)_{ub}^{l_m}} P_{m+1}(\tau^{m+1}|\tau^m) P_{m,nest}(\tau^m|k). \tag{19}$$

By interchanging the order of summation, we have

$$\sum_{\tau^{m+1}=\left(\left(k_{lb}^{l_1}\right)\cdots\right)_{lb}^{l_{m+1}}}^{\left(\left(k_{ub}^{l_1}\right)\cdots\right)_{ub}^{l_{m+1}}} P_{m+1,nest}(\tau^{m+1}|k) = \sum_{\tau^m=\left(\left(k_{lb}^{l_1}\right)\cdots\right)_{lb}^{l_m}}^{\left(\left(k_{ub}^{l_1}\right)\cdots\right)_{ub}^{l_m}} \left(\sum_{\tau^{m+1}=\left(\left(k_{lb}^{l_1}\right)\cdots\right)_{lb}^{l_{m+1}}}^{\left(\left(k_{ub}^{l_1}\right)\cdots\right)_{ub}^{l_{m+1}}} P_{m+1}(\tau^{m+1}|\tau^m) \right) P_{m,nest}(\tau^m|k). \tag{20}$$

By definition of the relative frequency (8), we have that

$$\sum_{\tau^{m+1}=\left(\left(k_{lb}^{l_1}\right)\cdots\right)_{lb}^{l_{m+1}}}^{\left(\left(k_{ub}^{l_1}\right)\cdots\right)_{ub}^{l_{m+1}}} P_{m+1}(\tau^{m+1}|\tau^m) = 1. \tag{21}$$

Thus

$$\sum_{\tau^{m+1}=\left(\left(k_{lb}^{l_1}\right)\cdots\right)_{lb}^{l_{m+1}}}^{\left(\left(k_{ub}^{l_1}\right)\cdots\right)_{ub}^{l_{m+1}}} P_{m+1,nest}(\tau^{m+1}|k) = \sum_{\tau^m=\left(\left(k_{lb}^{l_1}\right)\cdots\right)_{lb}^{l_m}}^{\left(\left(k_{ub}^{l_1}\right)\cdots\right)_{ub}^{l_m}} P_{m,nest}(\tau^m|k). \tag{22}$$

But $\sum_{\tau^m=\left(\left(k_{lb}^{l_1}\right)\cdots\right)_{lb}^{l_m}}^{\left(\left(k_{ub}^{l_1}\right)\cdots\right)_{ub}^{l_m}} P_{m,nest}(\tau^m|k) = 1$ by assumption. Therefore,

$$\sum_{\tau^{m+1}=\left(\left(k_{lb}^{l_1}\right)\cdots\right)_{lb}^{l_{m+1}}}^{\left(\left(k_{ub}^{l_1}\right)\cdots\right)_{ub}^{l_{m+1}}} P_{m+1,nest}(\tau^{m+1}|k) = 1, \tag{23}$$

which concludes the proof.

References

Azzalini, A., Capitanio, A., 1999. Statistical applications of the multivariate skew-normal distribution. Journal of the Royal Statistical Society, Series B 61 (3), 579–602.

Asakura, Y., Kashiwadani, M., 1991. Road network reliability caused by daily fluctuation of traffic flow. European Transport: Highways and Planning 19, 73–84.

Asakura, Y., Hato, E., Kashiwadani, M., 2003. Stochastic network design problem: an optimal link investment model for reliable network. In: Bell, M.G.H., Iida, Y. (Eds.), The Network Reliability of Transport: Proceeding of the 1st International Symposium on Transportation Network Reliability. Elsevier, Oxford, UK.
Azzalini, A., Capitanio, A., 1999. Statistical applications of the multivariate skew-normal distribution. Journal of the Royal Statistical Society, Series B 61, 579–602.
Bates, J., Polak, J., Jones, P., Cook, A., 2001. The valuation of reliability for personal travel. Transportation Research Part E 37 (2-3), 191–229.
Berdica, K., 2002. An introduction to road vulnerability. Transport Policy 9, 117–127.
Bell, M.G.H., 1999. Measuring network reliability: a game theoretic approach. Journal of Advanced Transportation 33 (2), 135–146.
Bell, M.G.H., 2000. A game theory approach to measuring the performance reliability of transport networks. Transportation Research Part B 34 (6), 533–546.
Bell, M., Cassir, C., 2000. Reliability of Transport Networks. Research Studies Press, London, UK.
Bell, M., Cassir, C., 2002. Risk-averse user equilibrium traffic assignment: an application of game theory. Transportation Research Part B 36 (8), 671–682.
Carey, M., Ge, Y., 2012. Comparison of methods for path flow reassignment for dynamic user equilibrium. Networks and Spatial Economics 12 (3), 337–376.
Chang, T., Nozick, L., Turnquist, M., 2005. Multiobjective path finding in stochastic dynamic networks with application to routing hazardous materials shipments. Transportation Science 39 (3), 383–399.
Chen, A., Yang, H., Lo, H.K., Tang, W.H., 2002. Capacity reliability of a road network: an assessment methodology and numerical results. Transportation Research Part B 36 (3), 225–252.
Clark, S., Watling, D., 2005. Modelling network travel time reliability under stochastic demand. Transportation Research Part B 39 (2), 119–140.
Cassir, C., Yang, H., Kakan, L., Tang, W., Bell, M.G.H., 2001. Travel Time versus Capacity Reliability of a Road Network: Reliability of Transport Networks. Research Studies Press, United Kingdom.
Coifman, B., 2002. Estimating travel times and vehicle trajectories on freeways using dual loop detectors. Transportation Research Part A 36 (4), 351–364.
Dion, F., Rakha, H., 2006. Estimating dynamic roadway travel times using automatic vehicle identification data for low sampling rates. Transportation Research Part B 40 (9), 745–766.
Fei, X., Lu, C., Liu, K., 2011. A Bayesian dynamic linear model approach for real-time short-term freeway travel time prediction. Transportation Research Part C 19 (6), 1306–1318.
Fu, L., Rilett, L., 1998. Expected shortest paths in dynamic and stochastic traffic networks. Transportation Research Part B 32 (7), 499–516.
Gut, A., 2009. An Intermediate Course in Probability, second ed. Springer, New York.
Haghani, A., Hamedi, M., Sadabadi, K.F., Young, S., Tarnoff, P., 2010. Data collection of freeway travel time ground truth with Bluetooth sensors. Transportation Research Record 2160, 60–68.
Härdle, W., Simar, L., 2007. Applied Multivariate Statistical Analysis, second ed. Springer, Berlin.
Herrera, J., Work, D., Ban, X., Herring, R., Jacobson, Q., Bayen, A., 2010. Evaluation of traffic data obtained via GPS-enabled mobile phones: the Mobile Century field experiment. Transportation Research Part C 18 (4), 568–583.
Heydecker, B.G., Lam, W.H.K., Zhang, N., 2007. Use of travel demand satisfaction to assess road network reliability. Transportmetrica 3 (2), 139–171.
Higatani, A., Kitazawa, T., Tanabe, J., Suga, Y., Sekhar, R., Asakura, Y., 2009. Empirical analysis of travel time reliability measures in Hanshin expressway network. Journal of Intelligent Transportation Systems 13 (1), 28–38.
Huang, H., Gao, S., 2012. Optimal paths in dynamic networks with dependent random link travel times. Transportation Research Part B 46 (6), 579–598.
Johnson, R., Wichern, D., 2007. Applied Multivariate Statistical Analysis, 6th ed. Pearson/Prentice Hall, Upper Saddle River, NJ.
Jula, H., Dessouky, M., Ioannou, P., 2008. Real-time estimation of travel times along the arcs and arrival times at the nodes of dynamic stochastic networks. IEEE Transactions on Intelligent Transportation Systems 9 (1), 97–110.
Karlaftis, M., Vlahogianni, E., 2011. Statistical methods versus neural networks in transportation research: differences, similarities and some insights. Transportation Research Part C 19 (3), 387–399.
Kharoufeh, J., Gautam, N., 2004. Deriving link travel-time distributions via stochastic speed processes. Transportation Science 38 (1), 97–106.
van Lint, J.W.C., Hoogendoorn, S.P., van Zuylen, H.J., 2005. Accurate freeway travel time prediction with state-space neural networks under missing data. Transportation Research Part C 13 (5–6), 347–369.
van Lint, J.W.C., 2008. Online learning solutions for freeway travel time prediction. IEEE Transactions on Intelligent Transportation Systems 9 (1), 38–47.
van Lint, J., van Zuylen, H., Tu, H., 2008. Travel time unreliability on freeways: why measures based on variance tell only half the story. Transportation Research Part A 42, 258–277.
Lo, H., Szeto, W.Y., 2002. A cell-based variational inequality formulation of the dynamic user optimal assignment problem. Transportation Research Part B 36, 421–443.
Lo, H., Luo, X., Siu, B.W.Y., 2006. Degradable transport network: travel time budget of travelers with heterogeneous risk aversion. Transportation Research Part B 40 (9), 792–806.
Lomax, T., Schrank, D., Turner, S., Margiotta, R., 2003. Selecting Travel Reliability Measures. Texas Transportation Institute, Cambridge Systematics Inc.
Miller-Hooks, E., Mahmassani, H., 2000. Least expected time paths in stochastic, time varying transportation networks. Transportation Science 34, 198–215.
Özbay, K., Kachroo, P., 1999. Incident Management in Intelligent Transportation Systems. Artech House, Boston.
Pattanamekar, P., Park, D., Rilett, L., Lee, J., Lee, C., 2003. Dynamic and stochastic shortest path in transportation networks with two components of travel time uncertainty. Transportation Research Part C 11 (5), 331–354.
Peeta, S., Ziliaskopoulos, A., 2001. Foundations of dynamic traffic assignment: the past, the present and the future. Networks and Spatial Economics 1 (3/4), 233–266.
Petty, K., Bickel, P., Ostland, M., Rice, J., Schoenberg, F., Jiang, J., Ritov, Y., 1998. Accurate estimation of travel times from single-loop detectors. Transportation Research Part A 32 (1), 1–17.
Sumalee, A., Kurauchi, F., 2006. Network capacity reliability analysis considering traffic regulation after a major disaster. Networks and Spatial Economics 6 (3–4), 205–219.
Sumalee, A., Zhong, R.X., Pan, T.L., Szeto, W.Y., 2011. Stochastic cell transmission model (SCTM): a stochastic dynamic traffic model for traffic state surveillance and assignment. Transportation Research Part B 45 (3), 507–533.
Sumalee, A., Wang, J., Jedwanna K., Suwansawat S., in press. Probabilistic fusion of vehicle feastures for re-identification and travel time estimation using video image data. Transportation Research Record.
Sun, L., Yang, J., Mahmassani, H., 2008. Travel time estimation based on piecewise truncated quadratic speed trajectory. Transportation Research Part A 42 (1), 173–186.
Taylor, M., Sekhar, S., D'este, G., 2006. Application of accessibility based methods for vulnerability analysis of strategic road networks. Networks and Spatial Economics 6 (3-4), 267–291.
Texas Transportation Institute and Cambridge Systems Inc., 2006. Travel Time Reliability: Making It There On Time, All The Time. <http://www.ops.fhwa.dot.gov/publications/ttreliability/index.htm> (retrieved 30.01.06).
Wen, Y., 2008. Scalability of Dynamic Traffic Assignment. PhD Dissertation. Massachusetts Institute of Technology.
Wu, C., Ho, J., Lee, D., 2004. Travel-time prediction with support vector regression. IEEE Transactions on Intelligent Transportation Systems 5 (4), 276–281.
Yang, H., Bell, M., Meng, Q., 2000. Modeling the capacity and level of service of urban transportation networks. Transportation Research Part B 34, 255–275.
Zhong, R., 2011. Dynamic Assignment, Surveillance and Control for Traffic Network with Uncertainties. PhD Dissertation. The Hong Kong Polytechnic University.